

1991

# The design and development of a U.S. Navy sonobuoy optical remote function select system

William L. Gelatka  
*Lehigh University*

Follow this and additional works at: <http://preserve.lehigh.edu/etd>

---

## Recommended Citation

Gelatka, William L., "The design and development of a U.S. Navy sonobuoy optical remote function select system" (1991). *Theses and Dissertations*. Paper 8.

This Thesis is brought to you for free and open access by Lehigh Preserve. It has been accepted for inclusion in Theses and Dissertations by an authorized administrator of Lehigh Preserve. For more information, please contact [preserve@lehigh.edu](mailto:preserve@lehigh.edu).

AUTHOR:

Gelatka, William L.

TITLE: The Design

and Development

of a U.S. Navy

Sonobuoy Optical

Remote Function

DATE: January 1992

THE DESIGN AND DEVELOPMENT OF A U.S. NAVY  
SONOBUOY OPTICAL REMOTE FUNCTION SELECT SYSTEM

by

William L. Gelatka

A Thesis

Presented to the Graduate Committee

of Lehigh University

in Candidacy for the Degree of

Master of Science

in

Electrical Engineering

Lehigh University

1991

Approved:

Dec 4, 1991  
Date

(Adviser

Dec 4, 1991  
Date

Chairman, Graduate Review Committe

## TABLE OF CONTENTS

	Page
CERTIFICATE OF APPROVAL	ii
TABLE OF CONTENTS	iii
LIST OF FIGURES	v
ABSTRACT	1
SECTION	
1.0 Introduction	2
1.1 Current Sonobuoy Procedures	3
1.2 Current Deficiencies	5
1.3 Requirements for a Remote Function Select System	6
1.4 Design Trade-off Analysis of an RFS System	8
1.5 The Optical RFS (ORFS)	9
1.6 Section Summary	11
2.0 The Laboratory Optical Remote Function Select	13
2.1 System Description	13
2.2 System Testing	23
2.3 Results	28
2.4 Section Summary	30
3.0 The Airborne ORFS	31
3.1 Analytic System Design	31
3.2 System Description	45
3.3 System Testing	55
3.4 Flight Test Results	65
3.5 Section Summary	67
4.0 Additional System Evaluation and Testing	68
4.1 Evaluation of Optoelectronic Devices	68
4.2 Evaluation of Optical Components	69
4.3 Section Summary	72
5.0 Improvements to the ORFS System	73
5.1 Modulation and Baud Rate Analysis	73
5.2 Frequency Shift Keying (FSK) Breadboard Modem	76
5.3 The New FSK Specification and Analytical Design	80
5.4 FSK Modem Testing and Evaluation	86
5.5 Response Time Tests	95
5.6 Miniaturation of Receiver/Transmitter	101
5.7 Aircraft Angular Alignment Measurements	105
5.8 Section Summary	106

6.0 A Preliminary Design for the Full ORFS System	107
6.1 System Overview	107
6.2 The R/T Matrix	112
6.3 The ORFS Modem Card	116
6.4 The ORFS Wand Assembly	120
6.5 Section Summary	122
7.0 Summary	124
7.1 Findings	124
REFERENCES	127
VITA	128

## LIST OF FIGURES

Figure		Page
1	Laboratory ORFS System Block Diagram	14
2	Laboratory ASK MODEM	16
3	Laboratory Interconnection	17
4	Laboratory R/T Assembly	18
5	Laboratory Inverted Logic MODEM	29
6	Airborne ORFS System Version 1	47
7	Airborne ORFS System Version 2	48
8	Airborne ASK MODEM	50
9	Airborne R/T Assembly	51
10	19,200 Baud FSK MODEM	78
11	1200 Baud FSK MODEM	85
12	Test Fixture Assembly	102
13	Miniature R/T Assembly	104
14	P-3C ORFS System Block Diagram	108
15	P-3C R/T Matrix Interconnect	114
16	ORFS System Modem Board	117
17	Programming Wand Assembly	121

## ABSTRACT

The U.S. Navy currently uses sonar buoys (sonobuoys) launched from aircraft to locate and track submerged submarines. The sonobuoys are manually programmed on the ground prior to insertion in the aircraft sonobuoy launch tube (SLT), to operate at the projected optimum depth, lifetime and radio frequency (RF) data transmission channel for the search area. As conditions change in the operation area, there is no way to reprogram the sonobuoys in flight for optimum operation.

The Optical Remote Function Select (ORFS) is a system which allows the operator to interrogate, program and verify these operational parameters as many times as required while the buoy is in the aircraft SLT. The ORFS system consists of a computer, a modulator/demodulator and an optical data link.

This thesis details the design and development, including results of laboratory and flight testing, of a single SLT ORFS system developed at the Naval Air Development Center. The report also details a complete system design proposed for the U.S. Navy P-3C aircraft and preliminary work done towards the verification of the ORFS system.



## 1.0 INTRODUCTION

Currently the U. S. Navy and other NATO countries use various types of sonar buoys (sonobuoys) dropped from aircraft when attempting to locate submerged submarines. For this report, a generic sonobuoy will be assumed which includes an acoustic transducer, a radio transmitter, and a long spool of wire which serves to tether the transducer at the selected depth and provides the signal path between the two units. The sonobuoys are packaged in sealed, cylindrical plastic containers (sonobuoy launch container (SLC)) approximately 5" in diameter and 40" in length. The SLC is loaded externally into an aircraft launch tube while the aircraft is on the ground. When the aircraft reaches the operating area, the sonobuoy is deployed from the aircraft so as to land in the water at an appropriate spot to listen for noise generated from the submarine. When the sonobuoy enters the water, a salt water battery is energized which triggers the inflation of a flotation collar. This collar keeps the radio transmitter floating on the water. The transducer is then released from the transmitter package and the transducer wire is payed out until the transducer sinks to the selected depth. The acoustic signal received by the transducer is converted to an electrical signal and sent up the wire. The radio

transmitter sends this signal over a VHF radio channel to the aircraft. The aircraft systems receive this signal and through various techniques attempts to determine if a submarine signal is present, and, if so, the location of the submarine. After a certain preset lifetime, the sonobuoy scuttles itself and sinks so as not to tie up the RF channels with sonobuoys that are no longer in optimum positions. This occurs through ocean currents moving the sonobuoy or the submarine transiting away from the area.

Because sound can be reflected at the interface of thermal layers, a submarine can acoustically "hide" from a poorly placed sonobuoy. It is imperative that the transducer be placed at the proper depth and in the proper location in order to operate at the most favorable (for the aircraft) signal to noise ratio.

### 1.1 CURRENT SONOBUOY PROCEDURES

During the aircraft preflight, an operational plan is formulated to include estimates of the submarine location or intended search area, the thermal properties of the water in the area, the sonobuoy patterns to lay, and the search pattern the aircraft is to fly. Once this

is completed, the required types and amounts of sonobuoys are drawn from inventory and transferred to the aircraft.

Older sonobuoys relied on mechanical switches to set parameters and a crystal to set the radio frequency (RF) channel. The newer sonobuoys utilize a microprocessor and thus have expanded capability to be programmed to operate in a certain configuration as required by the mission scenario. For this generic sonobuoy, these capabilities include the operating lifetime, the transducer depth, and the RF channel for the data link. This programming is currently accomplished with the sonobuoy electronic function select (EFS). The EFS consists of push buttons to change the parameters and a display to verify the parameters. The buttons and display are part of the sonobuoy and are accessible through a flexible urethane window on the SLC. After programming is completed, the sonobuoy is loaded into one of the sonobuoy launch tubes (SLTs). A table is generated by the loader to include the type and the operating parameters of each buoy loaded into each SLT. This table information is loaded into the mission computer which is programmed to keep track of the stores inventory. The tactical coordinator officer (TACCO) then

uses the mission computer to launch sonobuoys when required.

## 1.2 CURRENT DEFICIENCIES

The current procedure suffers from many deficiencies which result in less than optimal operation. The first bottleneck is the time it takes to program each sonobuoy. In the case of the Navy P-3C aircraft, there are 48 externally loaded SLTs that can be loaded; therefore, each of these 48 sonobuoys must be programmed. This individual programming wastes valuable time and is prone to error if the loader is not careful.

A major source of error is in the generation of the load table. If the loader is not careful in loading and generating the table, the TACCO will have problems trying to launch the correct buoy; and, of course the inventory will be in error.

When the aircraft arrives on station, the thermal properties of the water are verified by launching a bathythermograph (BT) buoy which profiles the water temperature. The overriding deficiency with the current system is that when the water thermal properties measured by the BT buoy are different than the predicted

properties, the aircraft cannot reprogram the sonobuoys for the optimum configuration. This problem occurs frequently because of lack of reliable information, or during transit, the aircraft is directed to a different operating area.

Another problem that frequently occurs is that some of the 99 available RF channels can become unusable, either through a failed aircraft receiver or through background RF interference. When this occurs, the sonobuoys pre-programmed to use those channels are rendered useless.

### 1.3 REQUIREMENTS FOR A REMOTE FUNCTION SELECT SYSTEM

The shortcomings described in section 1.2 drove the Navy to explore the possibility of developing a system that could interrogate, program, verify, and reprogram sonobuoys while they are still in the SLT. Some basic design requirements of the remote function select (RFS) system were formulated and are as follows.

a. The system must be reliable. If it is not, the operators cannot use the system and will not rely on the system when needed, and therefore, the whole effort is wasted.

b. The system must be small and lightweight because weight added to an aircraft is detrimental to the aircraft operational characteristics.

c. Aircraft currently in the fleet must be modified, therefore, the system should be easy to install and the design should be applicable to all ASW aircraft types.

d. The technique must be simple and inexpensive to implement in the sonobuoy because the sonobuoy is a use once only device, and the Navy uses thousands of units in a year.

e. Some Navy aircraft types are configured with 60 SLTs in a close packed arrangement, therefore, the link must have a high noise immunity between adjacent launch tubes.

f. The system must include a bi-directional link between the aircraft and the sonobuoy so that the sonobuoy can be interrogated to determine its type and setup for inventory and also any re-programming can be verified.

g. The system must not radiate any RF energy that an adversary could detect to determine the presence of the aircraft.

#### 1.4 DESIGN TRADE-OFF ANALYSIS OF AN RFS SYSTEM

Following the criteria of section 1.3, some initial techniques to link data between the aircraft SLT and the sonobuoy were tabulated and evaluated. These initial ideas included:

a. Electrical contacts

Contacts get dirty and corrode, reducing the reliability. It is also a packaging problem to bring signals out of the sonobuoy and through the SLC.

b. Induction Loops.

An induction loop could be wrapped around the SLT and a receiving loop installed in the sonobuoy. This technique is not optimum because of weight, complexity, adjacent noise immunity, and emissions.

c. RF Link.

An RF link between the SLC and the buoy is not feasible because of RF emissions and adjacent noise immunity.

d. Solenoids to push EFS buttons.

A quick and dirty technique is to use a solenoid to push the existing EFS buttons but this is perhaps the worst idea because of complexity, weight, alignment problems and lack of a verification technique.

e. Fiber Optic Devices

Initially optical fibers were considered as a mechanism to carry a data stream from a central optical transmitter (Light Emitting Diode (LED) or laser diode) to each launch tube. After considering the optical design and optical power budget, this technique was ruled out as too complex.

f. Optical Link

An optical link could be a technique that would conform to the requirements of section 1.3 if proper design is followed. This is the technique that was pursued and will be described in detail.

## 1.5 THE OPTICAL RFS (ORFS)

The idea of using an optical link to transmit a data stream from the aircraft SLT to the sonobuoy appeared to be a viable idea. The optoelectronic devices are



inexpensive and reliable. There are no RF emissions that could be detected. Also there is high noise immunity between adjacent launch tubes.

Some of the important design criteria for the initial specification are as follows:

a. Data Rate and Format

Because only the depth, lifetime, and RF channel are the parameters required to be programmed, the data link does not have to pass a large amount of data words; therefore, a slow channel rate of 300 baud was selected. A standard 8 data bits, one start bit, one stop bit and no parity bit word format was used.

b. Modulation Type

To keep the system simple, binary amplitude shift keying (ASK) modulation was used with a carrier frequency of 19.2 kHz. The ASK technique is defined as an inactive light state (light off) is interpreted as a logical '1' and an active light state (light on at 19.2 kHz frequency) is interpreted as a logical '0'.

### c. Optical Frequency

Infrared Emitting Diodes (IREDS) and IR detectors operating between 800 nm and 1000 nm are the preferred choice for an optical link. The detector is relatively immune from ambient light interference and both components are generally inexpensive.

These general guidelines were documented and a formal specification was generated by the Naval Avionics Center (NAC), Indianapolis, Indiana. This specification titled "SPD-22, REQUIREMENTS FOR THE SONOBUOY REMOTE FUNCTION SELECT" specified all the formal requirements and also included the guidelines specified above. Other requirements such as locations of the optical receivers and transmitters, dimensions, and word formats for each particular sonobuoy types were in the SPD-22 as well.

### 1.6 SECTION SUMMARY

Currently the Navy has a frequent problem of placing the correct sonobuoy in the correct position. But, since newer sonobuoys use microprocessors to control certain parameters, a solution to this problem can now be a proposed. The microprocessor controls the various functions and can be modified to accept data from a data link between the sonobuoy and aircraft so as to re-

program these functions and send a reply. Various techniques were evaluated and it appears that an IR optical data channel could provide the mechanism to link data between the aircraft launch tube and the sonobuoy. As a starting point, a specification was generated which needs to be evaluated in the real world.

## 2.0 THE LABORATORY OPTICAL REMOTE FUNCTION SELECT (ORFS)

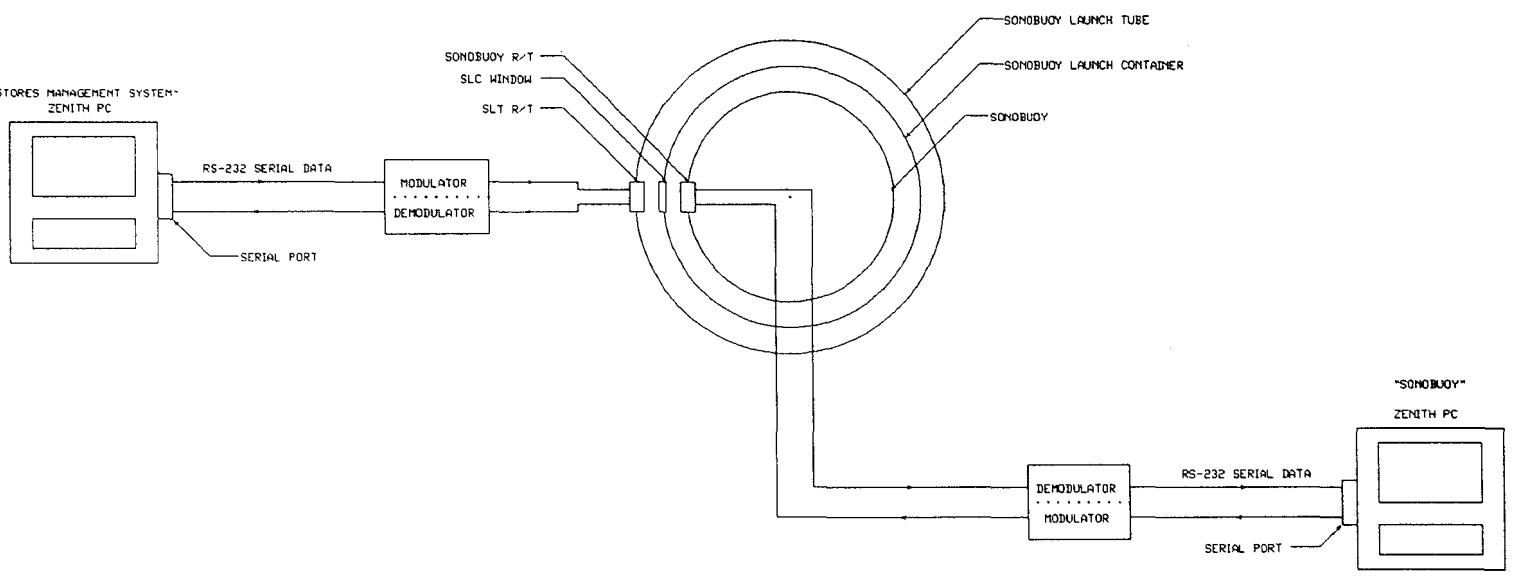
About December 1989, the Navy was about to commit to the development and production of a new anti-submarine warfare (ASW) aircraft, and the ORFS system would be included in the aircraft design. Before the Navy would agree to the development of a full ORFS system for this new aircraft, a laboratory proof-of-concept model was requested to be developed in order to evaluate the concept and determine any problems, and recommend improvements to the specification. This task, which includes the development, testing and evaluation of a proof-of-concept system, was assigned to the Naval Air Development Center (NADC), Laser/Magnetics Systems Branch. Because of the urgency of the task, the proof-of-concept system was designed almost entirely empirically using components that were on hand. A more formal design analysis is presented in section 3.1.

### 2.1 SYSTEM DESCRIPTION

A laboratory proof-of-concept system was developed in order to verify the operation of the optical link and the associated hardware in a simulated aircraft environment. As can be seen in Fig. 1, the system consisted of two personal computers (PCs), two modulator/demodulator (MODEM) boxes, along with

revisions			
zone	ltr	description	date measured

Fig 1 - Laboratory ORFS System Block Diagram



		NAVAL AIR DEVELOPMENT CENTER WARRINSTER, PA 18974	
		OPTICAL REMOTE FUNCTION SELECT LABORATORY PROOF-OF-CONCEPT BLOCK DIAGRAM	
prepared		size	code id
checked		no.	drawing no.
engineer		LEHMAN-FIG1 DMG	
GELATKA 10/24/91		scale	sheet

optoelectronic receivers and transmitters and their associated mounting fixtures and windows.

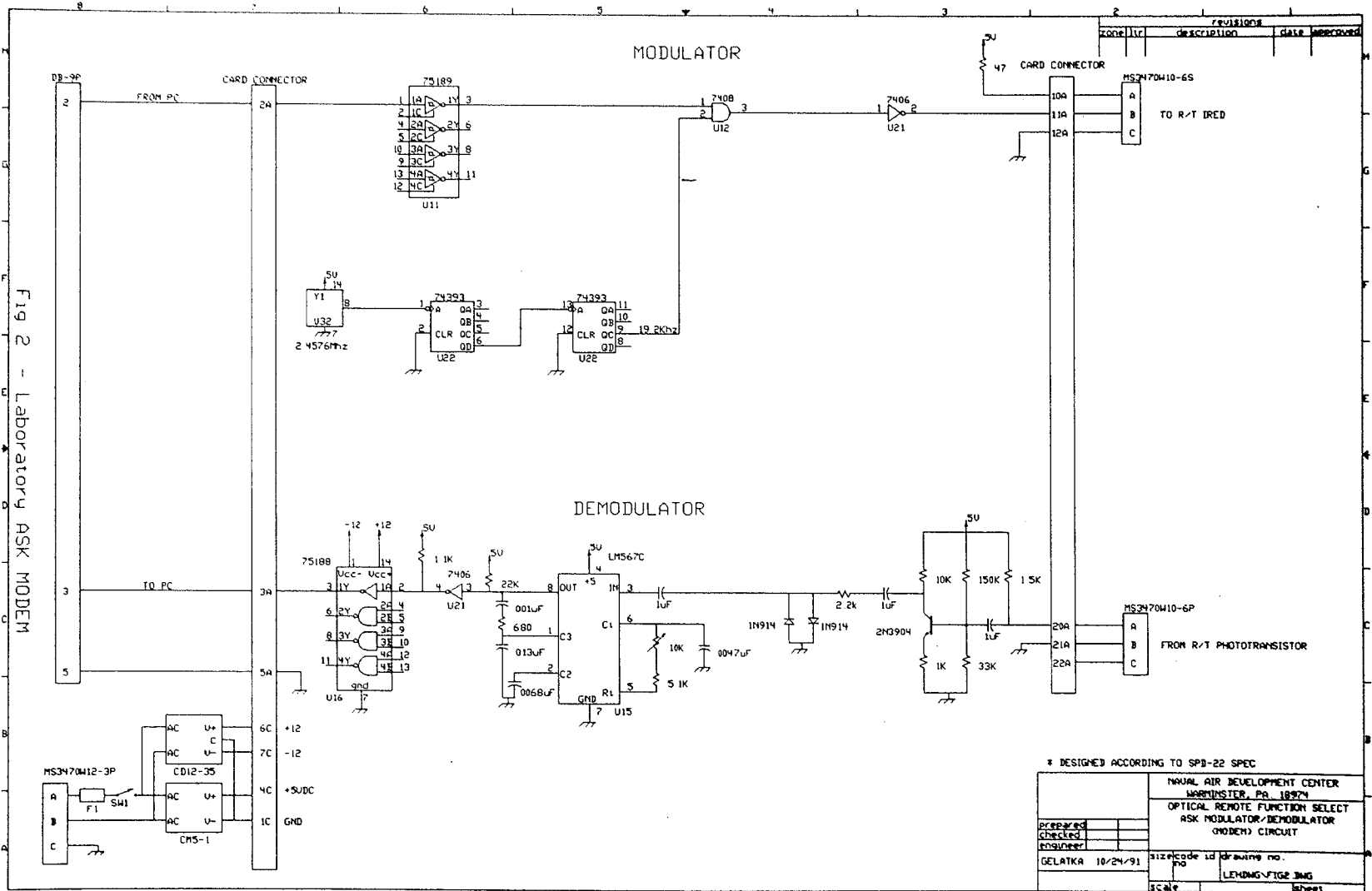
The stores management system (SMS) PC simulates the aircraft computer. This PC generates the message to send to the sonobuoy which is one of the messages defined by the SPD-22 specification. The message consists of 8 words of 8 data bits in length with one start bit, one stop bit and no parity bit at a 300 baud rate. This message is sent over an RS-232 serial channel to the aircraft MODEM box.

The MODEM box (Fig. 2) contains the ASK modulator and demodulator circuits. The serial data from the PC is received and ASK modulated. The ASK modulator circuit consists of a local oscillator and divider circuits to produce a 19.2 kHz carrier frequency. The carrier is gated with the data stream to produce the ASK modulated data stream. An open collector buffer inverter is used as a current sink for the IRED with a 47 ohm resistor as the current limiting resistor.

This drive signal is wired to the SLT receiver/transmitter (R/T) assembly (Fig. 3). The R/T assembly (Fig. 4) holds the IRED transmitter and IR

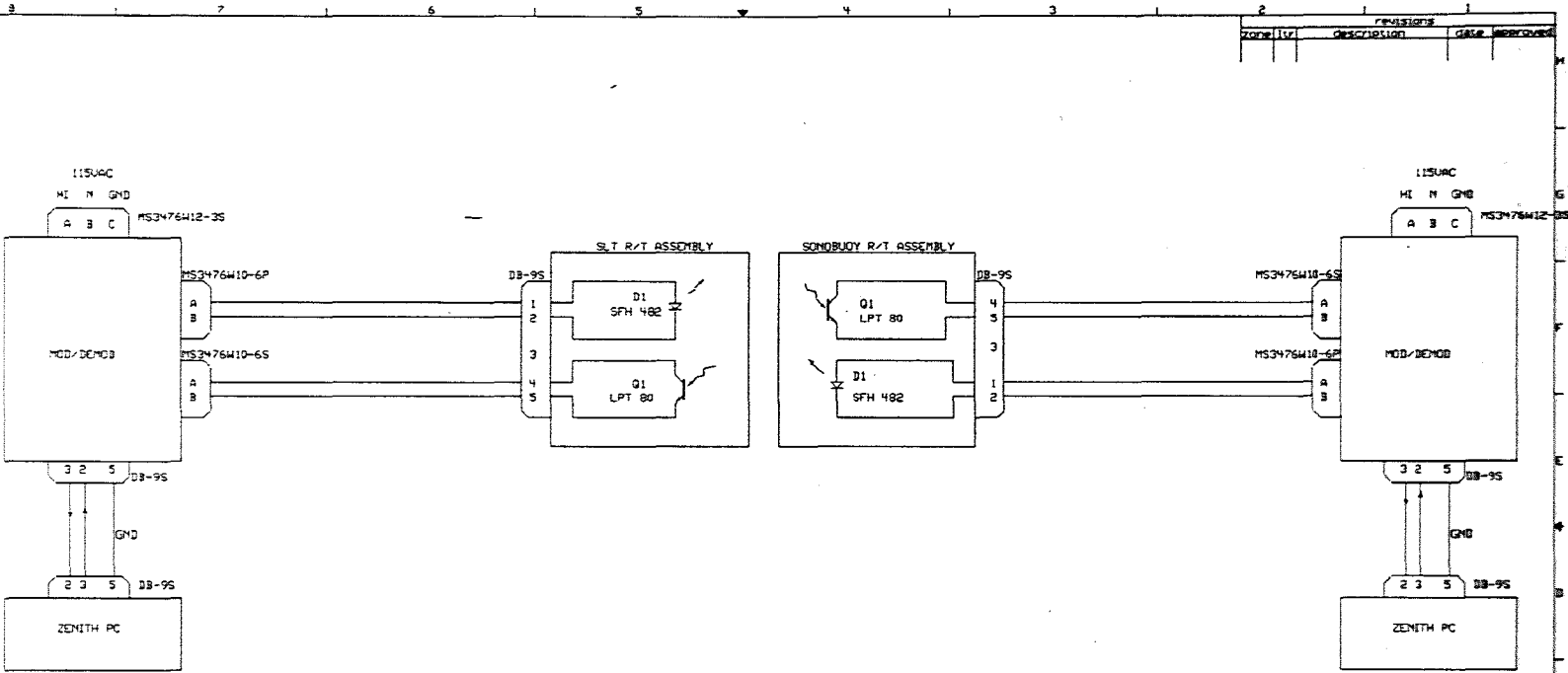
Fig 2 - Laboratory ASK MODEM

16



\* DESIGNED ACCORDING TO SP8-22 SPEC

NATIONAL AIR DEVELOPMENT CENTER WARRINSTER, PA 18074	
OPTICAL REMOTE FUNCTION SELECT ASK MODULATOR/DEMODULATOR (MODEM) CIRCUIT	
Prepared: _____ Checked: _____ Designer: _____	size/code id drawing no. PO _____ LEWIS-7122 3MG
GELATKA 10/24/91	scale: _____



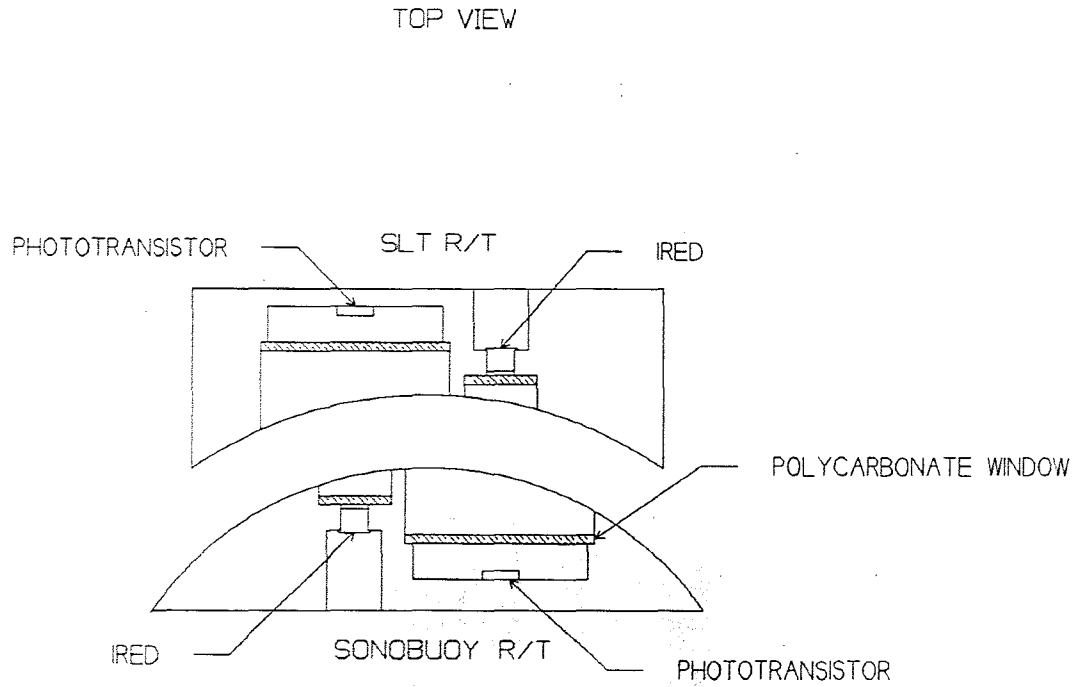
REVISIONS		
Zone/Qty	Description	Date/Issue/Rev

Fig 3 - Laboratory Interconnection

PREPARED CHECKED APPROVED		NAVAL AIR DEVELOPMENT CENTER WORMLESTER, Pa. 19379 OPTICAL REMOTE FUNCTION SELECT LABORATORY PROOF-OF-CONCEPT INTERCONNECT WIRING	
GELATKA 18/24/91		size/code of drawing no. PG. 18/24/91	
scale		sheet LEDGMS-VIG3.IMG	



Fig. 4 - Laboratory R/T Assembly



+

NAVAL AIR DEVELOPMENT CENTER WARRINGTON, PA 18984	
OPTICAL REARTE FUNCTION SELECT LABORATORY PROOF-OF-CONCEPT R/T ASSEMBLY	
DATE: 11/27/91	DESIGN NO. LEONG/F154.DWG
SCALE:	SHEET

phototransistor detector and was designed to allow the maximum clear viewing area for the receiver. The IRED for this experiment was a Siemens Components part number SFH 482 Gallium Aluminum Arsenide (GaAlAs) IRED. This IRED can provide 8 mW of radiated power at 880 nm wavelength with 100 mA forward current over a 40 degree (3 dB) half angle beam width. The on and off switching time ( $t_r$ ,  $t_f$ ) is on the order of 0.6  $\mu$ s which results in a maximum operating frequency of approximately 800 kHz. For this application, the IRED was not driven with the full recommended current. Approximately 60 mA of forward current was used which results in about 60% of the typical power output or 4.8 mW. This reduced power still provided exceptional results which are presented in section 2.2. The wide beamwidth was used to maintain operation with misalignment between the SLT transmitter and sonobuoy receiver. These limits are also presented in section 2.2.

The IR energy is transmitted through the transmitter acrylic (Plexiglass) window, through the urethane window of the SLC, and then through the receiver window where it finally reaches the receiver detector mounted in the sonobuoy R/T assembly. The detector is a phototransistor, Siemens LPT-80, which is designed to

receive, with high efficiency, radiation between 450 and 1080 nm. The peak sensitivity occurs at about 870 nm. This type of device will operate up to approximately 50 kHz which provides enough bandwidth for this experiment. This phototransistor was chosen because of the 40 degree half-angle acceptance angle of the device. This wide acceptance angle is necessary in order to operate with misalignment between the transmitter and receiver.

The electrical signal from the phototransistor is fed to the MODEM card where it is amplified by a discrete amplifier with a gain of approximately ten. The signal level is limited with diodes and fed to a phase-lock-loop tone (PLL) decoder integrated circuit (IC), National Semiconductor LM-567C. The tone decoder IC is basically a standard PLL device with the addition of a carrier detect output signal. This signal provides a saturated transistor switch to ground when an input signal is present within the passband.

The tone decoder circuit was designed to operate at a free running frequency ( $f_0$ ) of 19.2 KHZ. This is done by selecting  $R_t$  and  $C_t$  such that:

$$f_0 = 1/(R_t C_t)$$

and the recommended value of  $R_t$  is between 2 kOhm and 20 kOhm for best temperature stability.

The circuit was also optimized for speed of operation. The minimum lock-up time is related to the natural frequency of the loop. The lower the natural frequency, the longer becomes the turn-on transient. Thus, the maximum operating speed is obtained when  $C_2$  is at a minimum. This is done by selecting  $C_2$  and  $C_3$  according to the following expressions.

$$C_2 = 130/f_0 \quad \text{uF}$$

$$C_3 = 260/f_0 \quad \text{uF}$$

For  $f_0 = 19.2$  kHz this results in  $C_2 = 0.0068$  uF and  $C_3 = 0.013$  uF (0.015 uF standard value).

By selecting  $C_2$  at a minimum, the detection bandwidth is then the widest available. The typical detection bandwidth is specified as 14% of  $f_0$ . This results in a bandwidth of +/- 2.6 kHz around  $f_0$ . For this application, this bandwidth is acceptable because the expected carrier should not vary more than a few

percent and no noise signal is expected to be encountered within this bandwidth.

The minimum carrier cycles per data bit ratio at which digital information may be detected without information loss due to turn-on transient is specified by Signetics at about 10 cycles per bit and this was confirmed during the testing in section 3.3. For this experiment, the specification is 64 cycles per bit (19,200 Hz/300 bits per second) which means the PLL tone decoder circuit is more than adequate for this application.

The tone decoder circuit also incorporates output chatter prevention feedback circuitry. This circuitry prevents the output stage from transitioning through the threshold more than once. If multiple transitioning were allowed to happen, the logic circuits connected to the output would recognize the chatter as a series of ones and zeros which could result in message errors. The circuitry added to prevent output chatter includes a feedback resistor and capacitor which are added between the output and the lock detector filter capacitor ( $C_3$ ). This scheme operates by feeding the first output step

back into the input, pushing the input past the threshold until the transient conditions are over.

The demodulated signal is then fed to an RS-232 line driver for transmission to the sonobuoy simulator PC.

The sonobuoy simulator PC receives the message, checks for errors, and then sends a fixed reply message as defined by the SPD-22 to the SMS PC using an identical parallel path. When the SMS PC receives the reply message, the message is checked for errors, and the results are tabulated and displayed. The SMS message is then sent out again and the process continues until halted. Both PCs will always send the same message. Both units are programmed in a similar way to verify the received message against the expected message, and to display a running count of messages received and the number of bytes in error.

## 2.2 SYSTEM TESTING

The testing of the ORFS system was primarily geared to evaluate the concept of an optical link and to discover any problems associated with the present specification. The testing was limited to quantifying the optical dynamic range of the instrumentation, the

angular misalignment extent of operation, the influence of ambient illumination and the effects of light scattering due to environmental and operational conditions. The bit error rate (BER) testing was done to evaluate the optical link under simulated conditions as would be encountered in the real world.

The optical dynamic range was measured by introducing a series of neutral density filters into the light path between a transmitter and a receiver while conducting BER testing. Zero channel error was maintained up to an optical density of 1.1 where the system became "extremely" unreliable. This corresponds to an intensity reduction factor of approximately 13 (11 dB). Later tests with the airborne system resulted in a much higher dynamic range. Since this hardware was dismantled and certain parts were used in the airborne system (section 3), these earlier dynamic range tests could not be repeated to verify this result.

The SLC is held in the SLT by a set of mating tabs. To load a sonobuoy, the sonobuoy is inserted into the SLT and rotated approximately 45 degrees until the SLT anti-rotation latch locks into the SLC indentation. This anti-rotation latch prevents the SLC from rotating,

unlatching, and inadvertently falling out of the launch tube during flight. Because there is a range over which the SLC can rotate in the SLT, the ORFS optical link must accommodate this misalignment. The angular range of operation of the ORFS was measured by rotating the sonobuoy with respect to the SLT while measuring BER. The total angle of misalignment in which the ORFS would maintain 0 BER was 30 degrees, i.e., 15 degrees either side of center. When this testing was done, there was no specification given for this requirement; therefore, this allowable misalignment angle was assumed to be more than adequate to accommodate for misalignment. Measurements done at a later date (section 5.7) confirmed this assumption and placed a limit on the requirement for misalignment operation.

One of the concerns of using an optical link is the interference generated by ambient light which includes unmodulated light (sunlight) and 60 Hz and 400 Hz modulated light (artificial). The ORFS system was routinely operated in a brightly lit room without saturating the receiver and maintaining 0 BER. The light intensity, florescent lighting and sunlight, measured 200 microwatt/cm<sup>2</sup> (uW/cm<sup>2</sup>) @ 120 Hz and 1 milliwatt/cm<sup>2</sup> (mW/cm<sup>2</sup>) @ D.C.. These tests were conducted in an



environment much more severe than would normally be encountered in the aircraft with regard to ambient light illumination, because of the nature of the test fixture. In the test fixture, the transmitter and receiver are mounted close to the open ends of the tubes; this configuration allows for much more ambient illumination to arrive at the receiver. Additionally, the R/T assemblies have been operated under ambient illumination while dismantled. Plus, the initial breadboard testing was done with the IRED and phototransistor simply pointed at each other. Both configurations resulted in 0 BER. In conclusion, no problems were observed related to the normally encountered ambient illumination.

The effects of light scattering were determined in two simple tests which are related to the effects of long term use and environmental conditions. A plastic sheet was heavily abraded with 150 grit size emery cloth. This sheet was used to simulate the effects of abrasion on the optically transmitting surfaces between the IRED and detector. Signal continuity was maintained when this sheet was inserted between the R/T assemblies, although there were some problems associated with light being back scattered. This effect is addressed in the section 4.2.

Because the normal mission plan requires the aircraft to transition through various altitudes and operate in cold climates, the optical windows are prime candidates to accumulate frost build up. In order to simulate this effect, white 20 lb. bond paper was inserted between the R/Ts. In this configuration the ORFS system operated with 0 BER, however reflection problems similar to the aforementioned ones, were encountered.

The ORFS system was also turned over to an environmental testing group to characterize the effects of temperature extremes and temperature cycling. Additional tests with oil film and dirt build-up on the optical windows were also conducted. To quickly summarize the results, the ORFS system could not be made to fail during this testing.

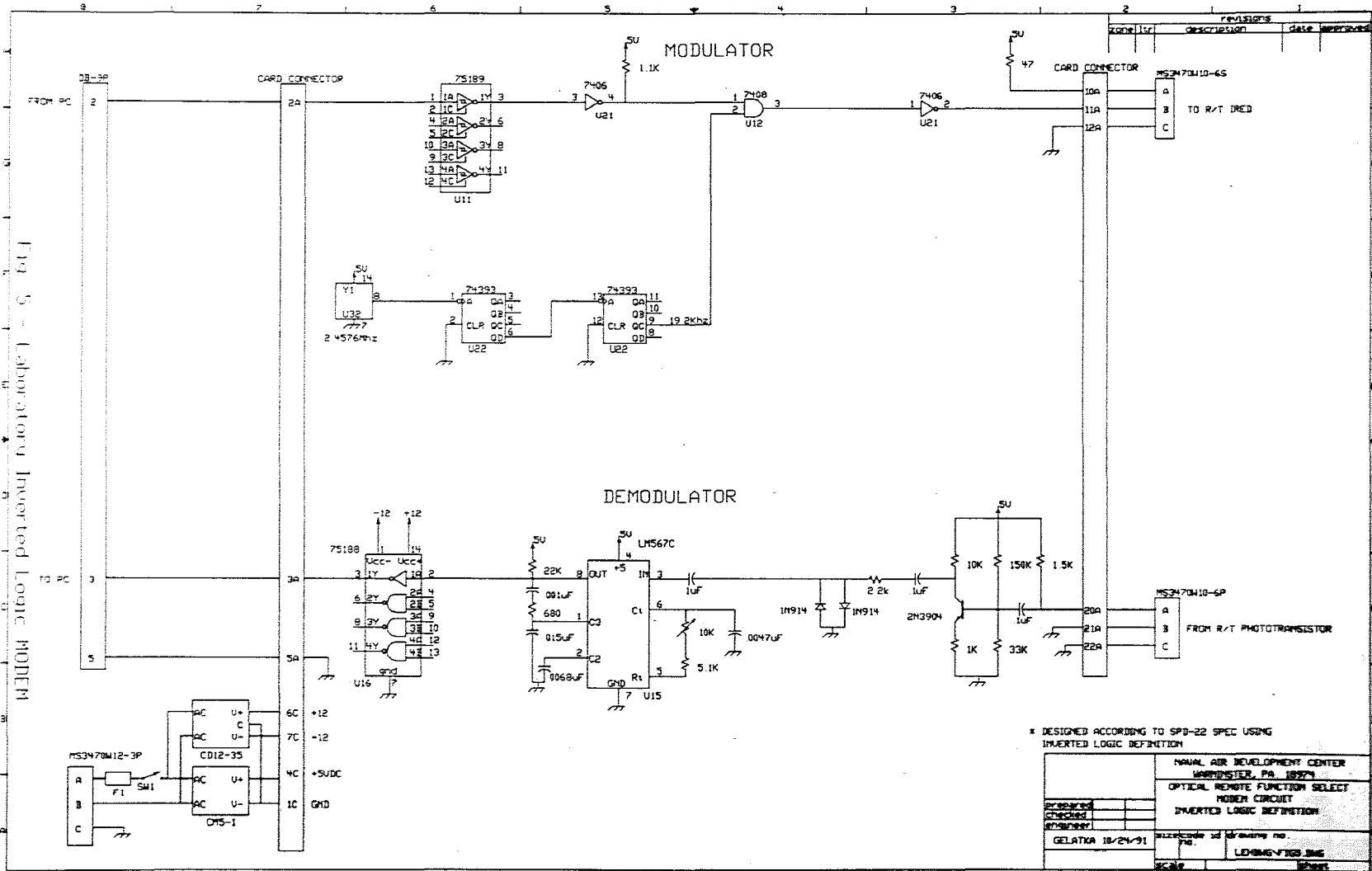
Even though the system performed well, the design and technique was not without faults. For instance, the initial specification calls for a logic 0, which corresponds to an idle state, as IRED active. It also defines some IRED turn-on time before the message and turn-off time after the message. A more straightforward approach was to invert the logical definition such that a

logic 0, which corresponds to idle, as the IRED inactive state. The MODEM was modified (Fig. 5) and the majority of these tests were rerun. The system operated as well as if not better than the initial configuration. The "better" performance was achieved during the frost and abrasion simulation tests because now only one transmitter is on at a time, reducing the chance of the R/T jamming itself with back-scattered light while trying to receive the true signal. This better performance is qualitative. It is based on the results of looking at the "cleanliness" of received signals; because in both cases the system achieved 0 BER.

### 2.3 RESULTS

The initial proof-of-concept ORFS system performed better than expected. The unit would routinely operate with 0 BER during various simulated conditions. The definition of 0 BER for this report is no errors in "hours" of continuous operation. The lack of errors resulted in the lack of taking true scientific data where the number of bits and the number errors would be recorded, graphed and statistically analyzed.

Fig. 5 - Laboratory Inverted Logic Modem



\* DESIGNED ACCORDING TO SP8-22 SPEC USING INVERTED LOGIC DEFINITION

Prepared		NATIONAL ASR DEVELOPMENT CENTER WARRINGTOWN, PA. 18771 OPTICAL REMOTE FUNCTION SELECT MODEM CIRCUIT INVERTED LOGIC DEFINITION
Checked		
Approved		
GELATICA 18/24-91		ALLICATED TO DRAWING NO. No. LEHMS-VTOS 886 SCALE: SHEET

## 2.4 SECTION SUMMARY

The ORFS system development was taken from initial specification to a working proof-of-concept model. In all tests that could be envisioned to simulate the real world, the system would routinely maintain 0 channel error. The concept was still in infancy and additional testing and evaluation still needed to be done to insure the reliability and applicability to the task.

While working with the system some peculiarities were discovered such as the logic convention previously reported. Others, which led to design change recommendations are reported in sections 4 and 5.

### 3.0 THE AIRBORNE ORFS

The success of the laboratory proof-of-concept ORFS system succeeded in converting most skeptics in the Navy to accepting the fact that an optical link could work in this application. The final proof of the technique would be to install the system in an aircraft and flight test the system. This next section describes the steps taken to redesign the system in order to accomplish the airborne testing.

#### 3.1 ANALYTICAL SYSTEM DESIGN

The initial system, because of time constraints and unfamiliarity with the pitfalls associated with an optical link technique, was designed almost entirely empirically on a breadboard trial and error basis. Learning from the previous experience plus having more development time available, a more formal analytical design approach could then be taken.

The standard approach for an RF data link analysis is to use the free-space propagation equation. This equation factors in the power out of the transmitter and the receiver sensitivity plus factors in all the gains and losses associated with antenna radiation patterns. A

similar approach, which is referred to as the flux budget, can now be used for the optical link design.

Analyzing the power out of the transmitter and the radiating pattern will be the starting point. The manufacturing process of IREDS results in devices with various power output levels for the same drive current. The devices are tested and a dash number is assigned to the basic part number to indicate the total power output available from the device. In order to stay on the conservative side, a low output power dash number IRED was chosen. Also, in the actual aircraft configuration, the transmitter and receiver are mechanically aligned to within a few degrees; therefore, a narrow beamwidth device could be used such as the Honeywell SE 5470-1 which is specified as 7 mW typical power output (at 100 mA  $I_F$ ) into a 10 degree half angle beamwidth.

Considering that the MODEM will consist of primarily digital TTL ICs, an open-collector TTL buffer would be assumed to drive the IRED. A typical TTL buffer will sink 40 mA of current at a guaranteed maximum output voltage of 0.8 V ( $V_{OL}$ ). Using these numbers, the load resistor can be calculated and a typical drive current and optical power output can be determined.

The load resistor is calculated from

$$R = (V_{CC} - V_F - V_{OL}) / I_F$$

where  $V_{CC} = 5 \text{ V}$  (typical TTL level).  $V_F$  is the diode forward voltage drop and varies with drive current. This relationship is characterized by the manufacturer and for a  $40 \text{ mA } I_F$ , the voltage drop is  $1.25 \text{ V}$ . The load resistor value therefore is  $74 \text{ ohms}$ . To be on the conservative side, a standard value  $100 \text{ ohm}$  resistor will be used which corresponds to about a  $30 \text{ mA } I_F$ . The emitted radiation of a GaAlAs IRED (and LEDs in general), in the normal operating range, changes linearly with forward current; therefore, a device operating at 30% of the rated  $I_F$  ( $30 \text{ mA}/100\text{mA}$ ), will output 30% of its rated optical power or  $2.1 \text{ mW}$  (30% of  $7 \text{ mW}$ ).

This optical signal must transmit through three windows and the losses with these windows must be factored into the equation. The signal loss, assuming transparent windows, is attributed mostly to reflection caused by differences in index of refraction between air and the window material. Using Fresnel's formula, which



solves for the reflection of light in a transparent medium in air, this reflection can be calculated.

If  $i$  is the angle of incidence,  $r$  the angle of refraction (measured from normal to the surface), the ratio of reflected light to incident light is given by

$$R = 1/2 \{ [\sin^2(i-r)/\sin^2(i+r)] + [\tan^2(i-r)/\tan^2(i+r)] \}$$

The beamwidth of the IRED is given as 10 degrees (0.17 Radians) half angle, also, the alignment of the transmitter and detector will maintain approximately normal incidence; therefore, for  $i$  near 0 (normal incidence), the small angle approximation for  $\sin$  and  $\tan$  could be used which is

$$\sin x = x \quad \text{and} \quad \tan x = x$$

which results in

$$R = 1/2 \{ (i-r)^2/(i+r)^2 + (i-r)^2/(i+r)^2 \}$$

which reduces to

$$R = \{ (i-r)/(i+r) \}^2$$

This equation needs to be put in terms of the index of refraction so that it can be solved for a reflection ratio. The index of refraction is an important parameter of materials and can be found in various chemical data books (CRC Handbook of Chemistry and Physics). Recalling Snell's law which is

$$n_1 \sin i = n_2 \sin r$$

where  $n_1$  and  $n_2$  are the index of refraction for the two mediums, and using the same small angle approximation, Snell's law reduces to

$$n_1 i = n_2 r$$

For air,  $n_1 = 1$  (approximately), therefore Snell's law reduces to

$$i = n_2 r$$

Substituting this into Fresnel's equation yields

$$R = \left\{ \frac{(n_2 r - r)}{(n_2 r + r)} \right\}^2$$

which reduces to

$$R = \{(n_2 - 1)/(n_2 + 1)\}^2$$

The index of refraction for thermoplastics range from 1.5 to 1.6 which result in 4% to 5% reflection from each surface, or 8% to 10% total loss per window.

Using the 10% (0.92 dB) loss figure from each window, the optical power at the detector will be reduced by 27% (2.75 dB) from the original 2.1 mW, or 1.5 mW.

This optical power must be converted to an irradiance value (H) or power per unit area, at the detector to determine the receiver signal level. The illuminated area may be determined by

$$A = \pi r^2$$

where

r = Aperture Radius

therefore it is necessary to determine the aperture radius. The distance (d) between the transmitter and

receiver is approximately 1 3/4 in. (4.5 cm.). The transmitter beamwidth is given as 10 degrees half angle (Phi). Using simple geometry,

$$\sin \text{Phi} = r/d$$

therefore

$$r = 4.5 \sin 10$$

or the radius is 0.78 cm.. The illuminated area is therefore 1.9 cm<sup>2</sup>. H at the detector is therefore 1.5 mW/1.9 cm<sup>2</sup> or 0.8 mW/cm<sup>2</sup>.

The output current of a phototransistor ( $i_{\text{ext}}$ ) is defined by

$$i_{\text{ext}} = i_{\lambda} (1 + h_{fe})$$

where  $h_{fe}$  is the common emitter gain of the transistor. The  $i_{\lambda}$  is the output current of a photodiode operating in the photoconductive mode (reverse bias with a bias voltage applied) and is defined as follows

$$i_{\lambda} = (n H A \lambda e) / (h c)$$

where

$n$  = Efficiency (# electrons out/# photons in)

$H$  = Irradiance

$A$  = Active detector area

$\lambda$  = Wavelength

$e$  = Electron charge

$h$  = Planck's constant

$c$  = Speed of light

In order to save the user from calculating this value, the manufacturers have tested their devices and provide this information in tables and charts. The importance of the above equation is the linear relationship between irradiance at the detector and current output. The deviation of this linear relationship between the irradiance and the photocurrent output is less than 20% and usually less than 10% over four powers of ten of photocurrent from some 100 nA (dark current) to some mA (near maximum device dissipation).

The light current specification value for the Honeywell SD 3443-1 is given as 0.5 mA minimum with  $H = 5$  mW/cm<sup>2</sup>. With the calculated irradiance value of 0.8 mW/cm<sup>2</sup>, from the typical performance curve of  $I_L$  vs  $H$ , the expected signal level should be 0.08 mA. To convert this current signal to a voltage signal a transimpedance

amplifier (see section 5.4) or a load resistor could be used. The load resistor used previously is 1.5 kOhm, which would result in a signal level of 120 mV.

The smallest detectable input voltage for the LM567 tone decoder is listed as 20 mV rms typical and guaranteed 25 mV rms (70 mV P-P) maximum. The optical link will therefore provide enough signal to operate the tone decoder and expected dynamic range of operation can then be calculated.

$$\text{Dynamic Range (dB)} = 20 \log V/V_r$$

The initial voltage level is 120 mV and the required voltage or reference voltage ( $V_r$ ) is 70 mV which yields a dynamic range of only 5 dB.

It is unknown what exact losses will be encountered in the real world, but, a 5 dB dynamic range is not very robust. An easy solution to implement for increasing dynamic range is to add a gain stage between the detector and tone decoder to amplify the output of the phototransistor. An amplifier with a voltage gain of 10 will provide another 20 dB of dynamic range which now results in a 25 dB receiver dynamic range. This is

theoretically possible because the photodiode will still be operating in the linear range with the optical input reduced by 20 dB.

The above statement must be verified over the entire Mil-Spec temperature range because as temperature increases, the dark current also increases. Assuming the optical signal is reduced by the calculated 25 dB receiver dynamic range, this effect would relate to a signal level of

$$-25 \text{ dB} = 20 \log(V_{\text{min}}/120)$$

or  $V_{\text{min}} = 7 \text{ mV}$ .

A 7 mV signal across the 1.5 kOhm load resistor equates to a 5 uA photocurrent. From the performance curves, the dark current at room temperature (25 C) and  $V_{\text{CE}} = 5 \text{ V}$  is typically 0.3 nA; therefore, the device operation is not limited by the dark current effects. This dark current increases rapidly with temperature and at 125 C, the dark current is typically on the order of 2 uA which is on the order of the minimum received signal level, but, this dark current signal can be filtered out by the pre-amplifier and the performance will not be

affected. An important consideration is that this dark current increases with transistor gain ( $h_{fe}$ ) and bias ( $V_{CE}$ ); therefore, this effect will have to be re-evaluated if these parameters change.

Getting back to increasing the receiver dynamic range, another option is to increase the drive current of the IRED. Remember the calculations were done with the IRED only operating at 30% of rated output, or 2.1 mW. Boosting the drive current to the recommended 100 mA will gain another 5 dB in optical power and because of the linear relationship between phototransistor optical input and current output, the detector signal strength should increase by 5 dB.

The 100 mA  $I_F$  is the recommended DC operating characteristic at 25 degrees C. ambient temperature. The ORFS system is a Mil-Spec system and is thus required to operate from -55 to +125 degrees C.. The above option thus needs to be evaluated with this in mind.

IRED power output ( $P_o$ ) increases with forward current ( $I_f$ ) which increases the power dissipation ( $P_d$ ) and chip junction temperature ( $T_j$ ), resulting in



decreased optical power output and device operating lifetime.

The relationship of chip junction temperature to operating conditions is

$$T_j = T_A + R_{th} P_d$$

where

$R_{th}$  = package thermal resistance - junction to ambient (C/W)

$T_A$  = Ambient temperature

For this case design,  $R_{th} = 370$  C/W and for a  $T_A$  of 125 degrees C, the maximum allowable  $T_j = 150$  C. From the above equation, the maximum power dissipation allowed with no heat sink is 68 mW. At a  $V_F$  of 1.3 V this corresponds to an allowable  $I_F$  of only 52 mA. This calculation is done for DC operation but the ORFS system always operates in an AC mode with roughly a 50% duty cycle. A peak  $I_F$  of 100 mA with a 50% duty cycle results in an average  $I_F$  of 50 mA and is therefore within the maximum operating limits just calculated.

As was mentioned, as the junction temperature increases, the optical output power decrease. This

effect is caused by the change in forward voltage drop with temperature of approximately  $-2.0 \text{ mV/C}$ . From the performance curves of power output verses case temperature, a change in case temperature from 25 C to 150 C would result in a 4 dB loss which would severely affect the initial dynamic range of only 5 dB. To compensate for this effect, a constant current source could be used to drive the IRED or one or both of the above mentioned techniques to increase dynamic range could be pursued. The easiest technique, with regard to added circuitry, is to add the gain stage in the receiver; therefore, this was the technique implemented in the design.

Another factor that affects the optical output of IREDS, and thus the dynamic range, is the length of operation or "aging" of the device. The radiant power emitted by IREDS (and LEDs in general) declines with increasing length of operation.

Increased device temperature or operating current (and consequently temperature) accelerates the degradation rate. The magnitude of the acceleration factor is related to the device structure, and also because the case heat sinking and packaging thermal

resistance have a direct effect on the actual chip operating temperature, these factors must also be factored into the degradation rate.

Using the message specification of 8 words per message and 10 bits per word at a 300 baud rate, this corresponds to a total transmission time of 0.27 sec/message. During a typical 10 hour mission, it is envisioned that at the minimum only two messages would be required (1 inventory plus 1 programming) thus the minimum time a IRED would transmit would be .54 seconds. Even if the estimated time was increased to 1 second per mission and considering the average airframe lifetime is 20,000 hours before retirement, this still only corresponds to 2000 seconds, or less than one hour of operation for the life of the airframe. Considering degradation is not even noticeable until 100s of hours of operation, (3 dB loss at  $10^5$  hours typically) this effect is negligible.

As was mentioned, the ORFS system must operate over the entire Mil-Spec temperature range; therefore, the tone decoder operation must be analyzed over this temperature range. The principle effects of temperature

are the center frequency and the detection bandwidth stability.

The center frequency stability is listed as 35 +/- 140 ppm/C. over the -55 to 125 C. temperature range. This relationship has been tested by the manufacturer and the worst case variation is listed as -1% change in  $f_0$  at 125 C.. The resistor and capacitor that set the  $f_0$  must also be factored into this stability. Carbon film resistors change value at +/- 100 ppm/C. This would equate to approximately a 1% change in value. Polystyrene capacitors have the highest stability with temperature at about +/- 1% over the full Mil-Spec temperature range. At worst case, the component variation would then change the  $f_0$  by 1%. The operating bandwidth is 14% of  $f_0$  (see section 3.3) and increases to approximately 15% of  $f_0$  125 C.; therefore, temperature will have little effect on the operation of the tone decoder.

### 3.2 SYSTEM DESCRIPTION

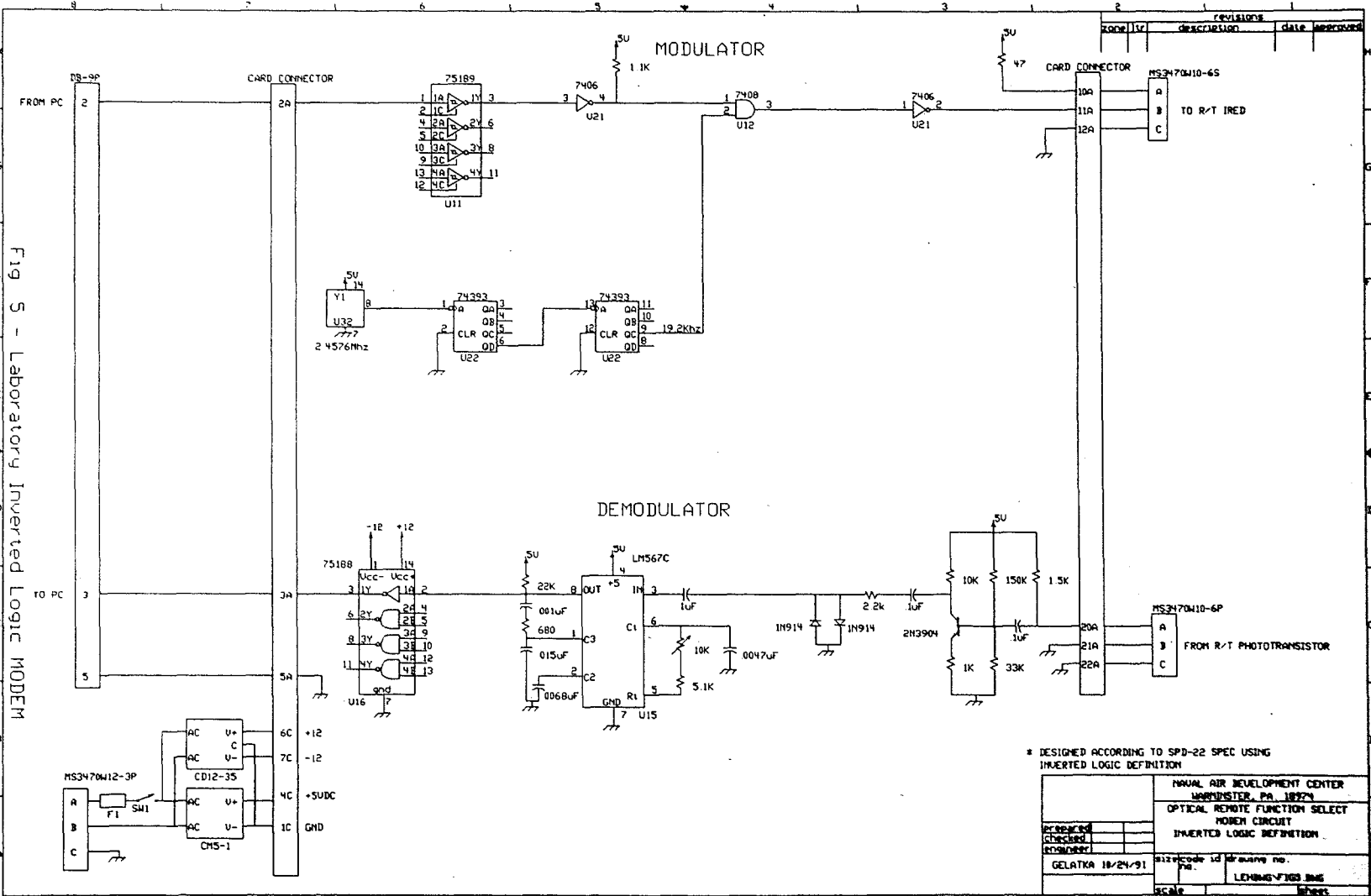
The laboratory ORFS system worked well and was an ideal configuration for laboratory testing and evaluation. An aircraft system requires a different design philosophy. The system should be as compact and

simple as possible. The use of two separate PCs and MODEM boxes was considered too involved in terms of physical size and operator convenience for an aircraft system; therefore, a new design was pursued.

An initial idea for the airborne system (Fig. 6) would use the existing MODEM and required the development of a simulator sonobuoy. This sonobuoy would contain an R/T assembly and circuitry to re-transmit the received message. It would also be battery powered. This idea was not received well because of projected design and operational shortfalls. The first and foremost engineering problem is associated with the packaging of the ORFS system in a sonobuoy tube plus operating from battery power. A dilemma would arise that if errors occurred in the messages during operational testing, then there would be no way to verify the source of the problem.

Another approach was developed which is shown in Fig. 7. As before, a portable PC would generate and receive messages. A MODEM box would ASK modulate and demodulate the data stream and provide the drive for the IRED and the bias for the phototransistor. A modified SLC would contain an R/T, but instead of having circuitry

Fig. 5 - Laboratory Inverted Logic Modem



REVISIONS		
NO.	DESCRIPTION	DATE APPROVED

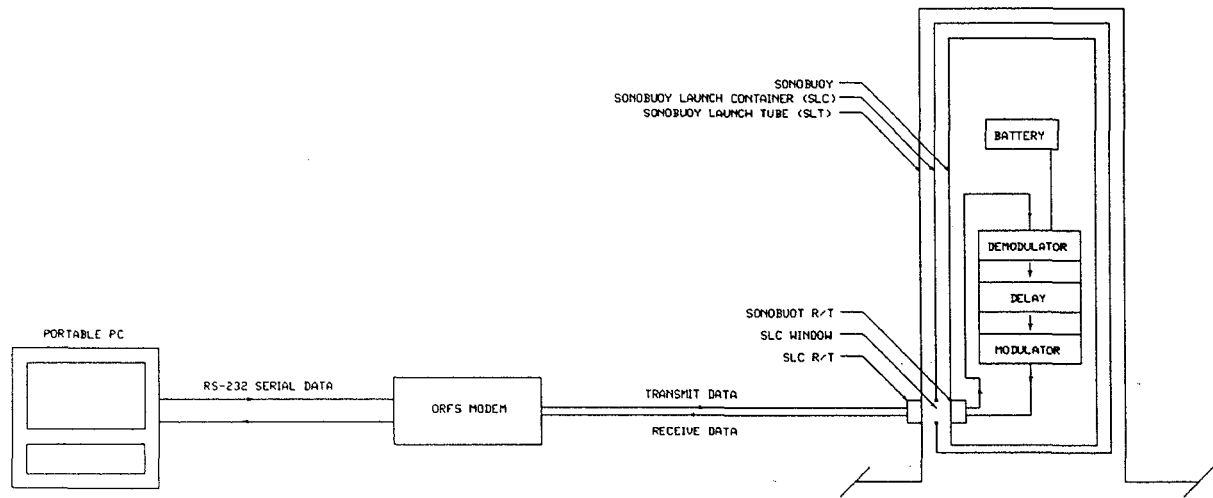


Fig 6 - Airborne ORFS System Version 1  
47

prepared checked released		NAVAL AIR DEVELOPMENT CENTER WORMLESTER, PA. 18924 OPTICAL REMOTE FUNCTION SELECT AIRCRAFT TEST SYSTEM VERSION 1	
GELATKA 10/24/91		size/code id/drawing no. no. LEHDMG-F106.BMG	
SCALE		REVISED	

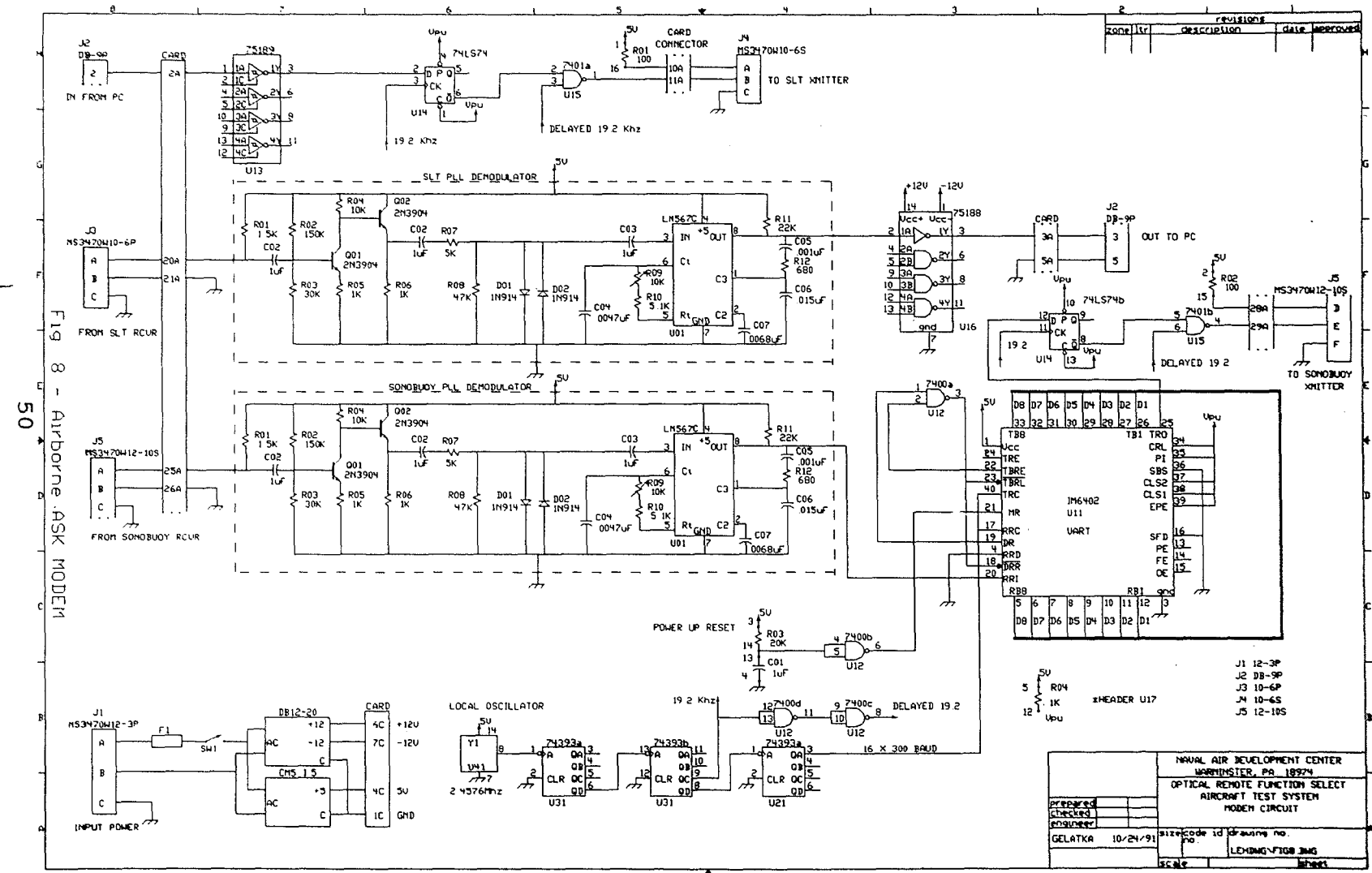
in the sonobuoy, the R/T signals would be wired directly to circuitry in the MODEM box.

Operationally, the system is quite similar to the laboratory system. A portable PC was used to generate and verify the messages but in a different format as will be described.

The message generated by the PC is sent to the ORFS interface box (Fig. 8) where it is received, modulated, and driven similar as before. The modulator circuit was modified in order to reduce the jitter in the demodulated data stream caused by the transient generated by the first cycle of the carrier. The local oscillator is not synchronized with the clock in the PC that is used to generate the data stream; therefore, the simple gating technique used previously would cause the period of the first cycle of the transmitted carrier to vary. A D type Flip-Flop was added to synchronize the data stream with the carrier. The results of this added circuit are presented in the test results of section 3.3.

The modulated signal is then fed to the IRED mounted in the SLT R/T (Fig. 9). The IRED used in this configuration is a Honeywell SE 5470-1. This device was





REVISIONS			
NO	DATE	DESCRIPTION	APPROVED

Fig 8 - Airborne ASK Modem

50

Prepared		size	code	id	drawing no
Checked					
Designed		GELATKA		10/24/91	LEHMANN-FIORE JMG
NAVAL AIR DEVELOPMENT CENTER WARRINSTER, PA 18974			OPTICAL REMOTE FUNCTION SELECT AIRCRAFT TEST SYSTEM MODEM CIRCUIT		

TOP VIEW

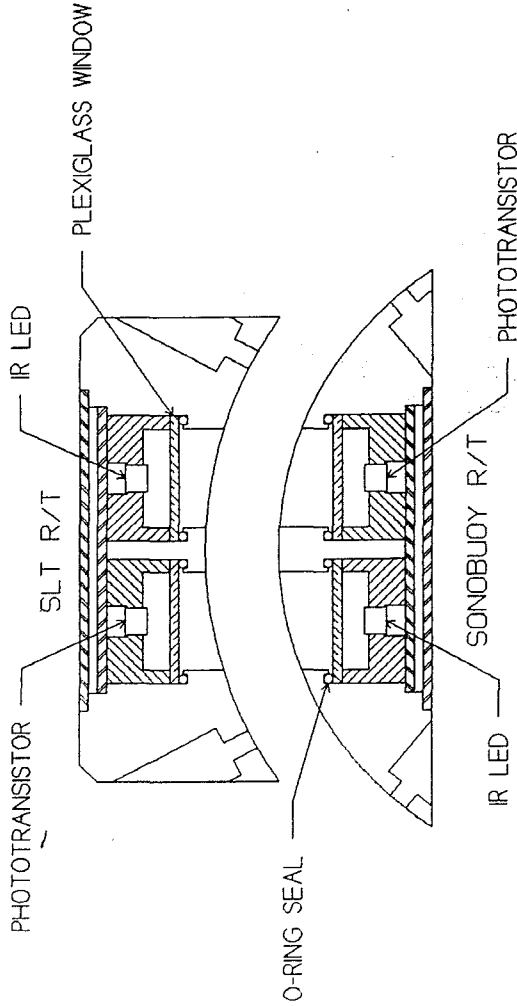


Fig. 9 - Airborne R/T Assembly

NATIONAL RESEARCH CENTER WARRINGTON, PA 15087	
OPTICAL DEVICE DIVISION SUBJECT AIRBORNE R/T ASSEMBLY	
DATE	DRAWING NO.
RELATKA 11/27/79	LE-500-2700-00
SCALE	HEET

used because it is a hermetically sealed, high-reliability IRED with similar characteristics (7 mW power output @ 100 mA forward current, 880 nm wavelength) to the laboratory IRED except for a narrower (20 degree full beamwidth at half maximum) beam angle. This narrower beam angle concentrates more power on the detector, but with a loss of misalignment tolerance. This tradeoff, as will be shown, is not a problem.

As before the IR signal transmits through the R/T window, the SLC window, then through the sonobuoy R/T window where it is received by the phototransistor. Again a high-reliability, hermetically sealed device was used (Honeywell SD 3443-1). This device is characteristically similar to the laboratory phototransistor except with a slightly wider acceptance angle of 45 degrees half-angle.

The received signal is then hard wire connected back to the MODEM box where it is demodulated with a tone decoder circuit. As a test, referring back to Fig. 8, an emitter follower amplifier was added to provide a drive stage (high input impedance, low output impedance) between the common emitter amplifier and the limiter diodes. This addition of this stage did not appreciably

affect the operation of the demodulator; therefore, the original laboratory demodulator circuit was used throughout the experiment.

From the results of the laboratory ORFS testing, it is highly recommended that the optical link operate in a half-duplex mode, which means only one transmitter and the matching receiver should be in use at one time. In order to accomplish this, the received message cannot not be immediately re-transmitted as it was being received, but instead needs to be delayed by the message length. To accomplish this, the message was shortened to one byte in length and a universal asynchronous receiver/transmitter (UART) was used as the delay element.

The demodulated message is loaded into the receive side of the UART in a serial fashion. When the complete word is received by the UART, the word is then parallel loaded into the transmit side of the UART and then serially sent to a modulator. This technique in effect produces a one word delay.

The message is then routed through a similar parallel path through the R/Ts back to the MODEM box for demodulation and then to the portable PC.

The PC was programmed to send a one byte message and wait for the return message. The program would then compare the received to the transmitted message and tally and display the transmitted byte count and the error byte count. The program also included a time out counter to restart if a word was not received in a fixed time and a re-synchronization function to restart the program if messages became out of synchronization due to catastrophic message errors.

Instead of sending a fixed message, one byte at a time, as defined by the SPD-22 specification, a different approach was taken. The PC sends one byte at a time and waits for a reply, starting with 00 HEX (all zeros) and increments by one until FF HEX (all ones) then back to 00 HEX to repeat the cycle. This technique thus checks all combinations of bits and is therefore a better test of the optical link. As an afterthought, a random number generator may have been a better engineering approach, but as will be shown, would probably not have affected the test results.

### 3.3 SYSTEM TESTING

The ORFS system was checked out in the laboratory prior to aircraft installation. From previous experience with the laboratory ORFS system, certain simple tests were performed to verify operation along with the normal signal measurements. As before, to verify operation with ambient light interference, the system must, and did, operate with 0 BER in the same well lit laboratory.

The dynamic range of operation of the system was measured and some interesting discoveries were made. The aircraft system would not operate with the laboratory frost simulator, 20 lb bond paper, between the optical paths as before. Voltage measurements at the receive, without any optical attenuation inserted showed that one receiver produced an output of a 1.25 V P-P signal while the other receiver only produced a 500 mV P-P signal. The aircraft and sonobuoy MODEM circuits were swapped and the signal levels remained associated with the R/T assemblies, ruling out any circuit differences with the MODEM circuits. A closer inspection of the IREDS showed differences in construction between the two devices. When looking into the lens of the IRED that produced less signal, the GaAlAs chip and leads could be plainly seen

as one view. With the IRED that produced more signal, the lens appeared to provide more magnification and only a partial area of the chip could be seen in one view. A side view showed a difference in the curvature of the lenses and therefore the overall length of the devices were different. The "high" power unit measured 0.245 in. while the "low" power unit measured 0.232 in. The catalog specifies a dimension of 0.224 in. to 0.247 in.. These devices therefore are within manufacturers specification and an even "lower" power device could be encountered. It is assumed from these results that the manufacturing tolerance of the lens affect the transmitted beam width and thus the signal received by the detector. An experiment was planned to measure the power output and characterize the beamwidth of a sample of IREDs, but instead, a manufactures test report concerning this exact problem was acquired. The manufacturers results, and a solution to this problem are presented further on in this section.

Once the cause of the signal differences was resolved, the IRED that produced the low signal was replaced. The "frost" experiment was repeated and the system operated successfully. Signal measurements showed the "new" IRED produced a 750 mV P-P signal at the

receiver without optical attenuation and with the "frost", the signal was reduced to approximately 20 mV P-P.

Remembering from section 3.1, the predicted received signal level should be on the order of 200 mV. This discrepancy is related to this manufacturing process and will be addressed further in this section.

Receiver sensitivity was then measured. The tone decoder circuit required approximately 100 mV P-P signal to assure reliable operation. This measurement is consistent with the tone decoder specification of 25 mVrms (70 mV P-P) typical detectable signal level. This translated to a measured signal level of approximately 15 mV P-P at the receiver front end. These numbers are approximate because of the noise on the signals at these low signal levels, it is hard to judge exact signal levels on an oscilloscope. A spectrum analyzer would have provided more exact measurements, but this experiment is only a proof-of-concept study and not an exacting test against a specification.



Using this receiver sensitivity of 15 mV and the maximum signal level received of 1.25 V, the dynamic range of operation of this circuit is then calculated.

$$\text{Dynamic Range} = 20 \log (1.25/.015) = 38 \text{ dB}$$

The prediction from section 3.1 for dynamic range was 25 dB. Remember the received signal level is on the order of 20 dB higher than predicted which would relate to a 45 dB dynamic range, but the guaranteed minimum detectable signal (MDS) level of the tone decoder was not reached by 7 dB which reduces the dynamic range back to the measured 38 dB. Not reaching the MDS can be attributed to power supply and circuit noise, which through better layout and construction practices, this noise could be reduced.

Of course by changing the IRED drive current and the demodulator pre-amplifier, the actual dynamic range can be varied. Qualitatively, if the system can operate with 20 lb bond paper between the optical components, the system should function properly in an aircraft environment.

In order to relate this system design to the irradiance and receiver sensitivity requirements of the specification, signal measurements were taken and "ball-park" calculations were done. The distance between the transmitter and detector is approximately 1 3/4 in. (4.5 cm.) Assuming the transmitter beamwidth is 10 degree half angle, which is highly suspect, again using simple geometry the illuminated area then at the detector is 1.9 cm<sup>2</sup>. The voltage across the load resistor was measured and the I<sub>F</sub> calculated which resulted in the output power level of 2.5 mW. The loss associated with the windows is 2.75 dB which reduces this level to 1.8 mW. Assuming this power is concentrated and evenly distributed in this area, then the irradiance at the detector with the optical attenuation is 0.95 mW/cm<sup>2</sup>. From the dynamic range measurements, the power output could be reduced by 38 dB and still maintain operation. This then corresponds to an irradiance of 0.15 uW/cm<sup>2</sup>. This value appears highly suspect but will be used in further calculations.

The SPD-22 specification for receiver sensitivity is given as 3.7 uW. Using the results above, and given that the active area of the phototransistor is specified as .65 mm<sup>2</sup>, the receiver sensitivity at minimum signal is

therefore 1 nW, which again appear highly suspect because it is such a low value.

In order to complete the calculations and knowing the irradiance at the detector, the agreement between the calculated received signal strength and the measured received signal strength can be shown. The quantum efficiency for this device is not given, but a graph of irradiance vs. photocurrent is given. The lowest irradiance value given is  $0.05 \text{ mW/cm}^2$ ; but remembering the linear relationship between irradiance and photocurrent the slope of the graph can easily be calculated and the graph can be extended to the calculated value and the photocurrent value can then be solved. The calculated irradiance value of  $0.15 \text{ uW/cm}^2$  should yield a photocurrent of about 20 nA which through the 1.5 kOhm load resistor translates to a signal level of 30 uV. The measured signal level was 15 mV which means the calculated value is 500 times too small.

As was discovered previously, the IRED beamwidth appeared highly variable. After receiving some applications notes from the manufacturer, this discrepancy can be explained. The application note states "Since only the total power is known, the power

for surfaces smaller than the total beam cannot be determined. Also ... light flux density is not predictable because of aberrations caused by the package and lens variables. Each application almost has to be designed empirically."

The application note also included output pattern plots for various packages. For the device in question, SE 5470, the two sigma limit for beam angle (full angle, 1/2 power) is given as a low of 4.7 degrees to a high of 20 degrees and the beam centering can be 0 degrees to 4 degrees from mechanical center. Using the minimum angle of 4.7 degrees and the maximum of 20 degrees, the power variation with respect to this angle could be shown. With a 4.7 degree beamwidth at the 4.5 cm. distance, the aperture area is  $0.1 \text{ cm}^2$ . Using the above total power of 1.8 mW, this relates to an irradiance of  $18 \text{ mW/cm}^2$  which is a 13 dB difference from the initial calculation. Of course the initial assumption of a uniform optical power in the aperture area is also a bad assumption; therefore, from this information, it is impossible to accurately calculate receiver sensitivity. Also because of such wide variations, this narrow beamwidth device could also cause erroneous receiver sensitivity measurements. This device should not be used in final designs.

The beamwidth for a device without a focusing lens is listed as 90 degrees and is better behaved. The beamwidth variation is measured at 88 degrees to 93 degrees. Some simple design calculations can be done to evaluate the applicability of these wide angle transmitters. The power output rating of these devices is 7 to 14 mW. Taking the lower number at the 4.5 cm distance and assuming only half of the power reaches the detector plane, this equates to  $0.05 \text{ mW/cm}^2$ . At this irradiance, a high sensitivity phototransistor detector such as a Siemens BPX 43 or the Honeywell SD 3443 will output about 50 uA of signal. Through a 1 kOhm resistor this equates to a 50 mV signal. This equates roughly to the minimum signal level required for 0 BER in the present system.

By selecting the higher power device, 3 dB signal gain can be achieved. By moving the transmitter and receiver closer together to 1 inch (2.5 cm) another 5 dB can be gained. This now relates to an irradiance of  $0.35 \text{ mW/cm}^2$ , (the specification calls for a minimum of  $0.2 \text{ mW/cm}^2$ ). At this level the phototransistor output would be approximately 300 uA which translates to 300 mV at the amplifier front end. By increasing the gain of the

amplifier, similar performance results can then be achieved. Of course these calculations are only rough and should be backed up with experimental results, but these results do at least show that those IRED devices without focusing lenses could be used for future designs and should provide more predictable results.

Tests were run with such a device using the FSK MODEM and are reported in section 5.4.

Another test was done in order to characterize the operation of the ASK demodulator. The Signetics data book defined a delay of up to 10 cycles of the carrier before the signal appeared at the output due to transient effects. This effect is caused because the PLL has a free running VCO not synchronized to the incoming carrier and the loop takes time to lock to the carrier when first applied. The minimum lock-on time occurs when the VCO frequency happens to be close to the phase of the carrier when it arrives. By the nature of the PLL, when the signal is first applied, the phase may be such as to initially drive the VCO away from the incoming frequency rather than toward it. When this happens, which of course is unpredictable, the lock-up transient is at its worst and will take longer for the transient to die out.

To measure this effect, a signal generator was substituted for the PC as the data source and the output of the tone decoder was monitored. The baud rate is given as 300 bits per second. Considering that the highest frequency data stream that could be generated is an alternating string of "ones" and "zeros", the frequency of this stream therefore corresponds to 150 Hz square wave. The generator was then set to operate at 150 Hz square wave output and varied about this frequency. As was expected, by dithering the square wave frequency, the number of cycles of carrier until the decoder detected the input signal varied in a beat frequency type fashion. Typically the minimum number of cycles measured was three cycles and the maximum number measured was eight cycles which is within the specification of 10 cycles.

There is also a fixed turn off delay that is not dependent on the data stream frequency but is related to the output filter capacitor. For this application a delay of approximately 200  $\mu$ S occurs.

Mechanical measurements were taken to evaluate the extent of mechanical rotational limits between the SLT

anti rotation latch and the SLC indentations for the P-3C aircraft. A limited sample showed the SLC could rotate +/- 1.3 degrees. The alignment error between the sonobuoy and the SLC is unknown. This error is judged to be minimal because of the mechanical assembly details that rely on alignment pins to maintain alignment of the sonobuoy in the SLC. Rotational testing was done on the airborne R/Ts which showed the system will work to +/- 11.5 degree misalignment with 0 BER.

The ORFS system was then ground tested in the aircraft. The ORFS sonobuoy was loaded in the aircraft SLT and the system was set up and operated. The buoy was positioned to contact all mechanical stops in order to verify performance within all SLT to SLC normal mechanical latching limits. The buoy was shaken as best as can be done to evaluate any vibration problems. No errors occurred in this half hour of operational ground testing.

#### 3.4 FLIGHT TEST RESULTS

The project flight was patterned after a typical mission. The aircraft would transit to a search area, simulate searching, localizing, tracking and attacking a target.



The aircraft transited to the operation area at a high altitude (20,500 ft) for approximately 30 minutes with the system operating to cold soak the system (-16 degrees C). The aircraft then stepped down in altitude until 250 ft above ground level (AGL) was reached. At this altitude moderate turbulence was encountered. After approximately 30 minutes at this altitude, the aircraft climbed to altitude (8,000 AGL) and returned to base. The system also operated during the landing and the taxi to the parking spot.

To summarize, the ORFS system was subjected to temperature, altitude, and power level changes, plus vibration and buffeting. The system operated continuously for 3 hours and 20 minutes, from ground to 20,500 ft and from 8 degrees C. to -16 degrees C. During the flight, 153,000 bytes were sent and received with a 0 BER.

The ORFS system flight in no way represents a complete flight test program. The test only shows that an optical link concept can operate in an aircraft environment.

### 3.5 SECTION SUMMARY

Even though the laboratory proof-of-concept ORFS system worked perfectly, there are those people that need proof that an aircraft system works in the actual aircraft environment. This request led to further development of the ORFS system. An analytical system design was presented and tests results were presented to verify, and point out the poor assumptions of the design. After the lab and aircraft ground testing, a single flight was flown patterned after a typical mission. The success of the flight furthered the interest of the ORFS system, though from an engineering standpoint, there are still some design issues to resolve such as the optical power levels and beam patterns.

#### 4.0 ADDITIONAL SYSTEM EVALUATION AND TESTING

The main objective of the previous work was to determine the applicability of an optical link to the sonobuoy remote function select task. As a separate task, various optoelectronic devices (IREDS and detectors) and optical components (filters and optical window materials) and their juxtaposition were evaluated. This testing was done to provide reference data for expected future design issues.

#### 4.1 EVALUATION OF OPTOELECTRONIC DEVICES

A major concern of the ORFS system in the present configuration is the amount of real estate and weight devoted to the R/T assemblies. Some ideas on how to reduce this area were pursued. The first idea to reduce size was to evaluate a component with an IRED and phototransistor mounted in a miniature plastic package (Siemens SFH-900). This component is a reflex light barrier detector for short distances. It is typically used as a position reporting device and end position switch in industrial and home electronics environments. This particular component is representative of a class of devices made by various manufacturers.

A pair of these components were evaluated on a ASK breadboard circuit with poor results. This type of device is primarily used in short distance applications (< 5 mm) and therefore little attention is paid in the beam forming design. The IRED is also a low power device and because of the lack of beamforming, spreads the IR energy over a large area (wide beamwidth) which results in little energy reaching the opposite receiver. This particular type of device is a poor candidate for the ORFS system. A device with a higher power IRED and beamforming could be a possibility.

The next configuration evaluated located the optical components in an R/T as close as possible to each other. The design and results of this experiment are reported in section 5.3.

#### 4.2 EVALUATION OF OPTICAL COMPONENTS

The laboratory testing also included the evaluation of various window materials. The current optical window was made of clear 1/16 inch acrylic (Plexiglass) and approximately 10% attenuation to the IR beam was measured. The measured values for acrylic and polycarbonate samples were on the order of 10% which show

good agreement with the calculated values from section 3.1.

Evaluation of SLC window films was also done. As a base line, the SLC window film that covers the EFS push buttons and display was tested. This film showed approximately a 9% loss. Various other urethane films from J.P. Stevens & Co., Northampton, MA. were also evaluated. The best (least attenuation) product is the clear material currently used in the SLC. The worst was an orange translucent film. The orange film was evaluated as an ambient light filter. The IR attenuation was measured at greater than 50% and little was gained as an ambient light filter; therefore, this product was deemed not acceptable. Clear translucent films of various grades were also evaluated. The attenuation with these films ranged between the clear film (9%) and the orange translucent film (56%).

Although there have been no problems operating the ORFS system in ambient light, it was still decided to investigate the effects of daylight filters on the operation of the system for future reference. The filters were obtained from Schott Optical, Duryea, PA.. Since the ORFS operates at 880 nm, the three filters

chosen attenuate throughout the visible region to 715 nm (RG-715), 780 nm (RG-780) and 830 nm (RG-830). These filters are all glass material of 1 mm in thickness. These filters reduce the light intensity throughout most of the visible region to less than 1%.

No appreciable performance improvements were achieved when these filters were installed in the ORFS system. The modulated signal was reduced by 8% with these filters. The sunlight (DC) and room lighting (120 Hz) effects were not appreciably affected by the filters. This can be explained because the signal at the demodulator is AC coupled and these effects are outside of this AC bandwidth. Also the phototransistor response is reduced to about 60% at 700 nm (red) and to 10% at 400 nm (violet). In the laboratory measurements, only bright sunlight directly illuminating the unfiltered phototransistor caused receiver saturation. This saturation could not arise while the sonobuoy is in the SLT.

When the sonobuoy is not in the shipping container or SLT, in order to prevent any inadvertent activation or current drain of the sonobuoy caused by visible ambient illumination, a photodiode with a built in visible light

cut-off filter could be used. These devices are resin molded using a black epoxy resin. In a typical phototransistor, Sharp PT380F, the spectral sensitivity response peaks about 880 nm with 0% transmission below 700 nm (visible region). All other characteristics are similar to previously used devices; therefore, there should be no problem using such a device. This type of package is not Mil-Spec approved and would not be usable in the aircraft R/T, but a device of this type could be used in the sonobuoy and would provide for a more robust system performance for no additional cost.

#### 4.3 SECTION SUMMARY

Because the ORFS is a new system and this technique was never attempted in an aircraft environment before, evaluation of various optical components was done to characterize the effects. This evaluation included different optoelectronic devices and optical window materials and filters. Though only a limited sample of devices were evaluated, this still provides the beginnings of a data base that future designs can draw from.

## 5.0 IMPROVEMENTS TO THE ORFS SYSTEM

The previous tests have shown that an optical link could be used to transfer data between the aircraft and the sonobuoy. Even though the system would routinely achieve 0 BER, the overall system design was considered far from optimum. The knowledge learned from previous tests plus new requirements on the system forced a re-evaluation of the system design criteria.

### 5.1 MODULATION AND BAUD RATE ANALYSIS

Once it was made known in the Navy community that data could be transferred from an aircraft to a sonobuoy and back, various other sonobuoy programs looked at how ORFS could be used in their application. One advanced sonobuoy program projected using the ORFS system to load computer algorithms into "smart" sonobuoys presently under development. The major shortfall of the ORFS system for this project is the relatively slow data rate. The advanced sonobuoy project would need to transfer a "large" amount of data in a timely manner. This request led to the re-evaluation of the data link speed and modulation type.

The operating speed of all components in the previously developed ORFS system were evaluated. The



result of this analysis is that the present system is already at or very near the maximum operating limit. The limiting component is the phototransistor used as the detector. High sensitivity phototransistors in general are only specified to operate up to approximately 80 kHz with reduced output. The present system is operating at 19.2 kHz. Above this frequency, loss of signal response was observed. The solution to this detector speed limitation is to substitute a photodiode detector. Photodiodes generally are at least 10 times faster, but have 100 to 1000 times lower photosensitivity (10s of microamps vs. milliamps output) than a phototransistor for the same optical input. As a breadboard test, a photodiode, Honeywell SD 3421, was substituted into the circuit and an OP-AMP (TL-071) circuit with an inverting gain of 100 was added as a pre-amp to the original demodulator circuit. The system in this configuration worked as well as the original design.

The next limiting component is the LM-567C PLL tone decoder with a typical operating frequency of 500 kHz.

Assuming that ASK is the modulation scheme to be used, then to boost the baud rate, the carrier frequency must be increased by a corresponding amount. If the same

number of cycles per bit (64) is maintained, then a 4800 baud data rate with a 307 kHz carrier would be the next physical limit, assuming the same PLL tone decoder is used. As an option, reducing the cycles per bit to 32, which is still within the minimum PLL operating specification of 10 cycles per bit, the system could obtain 9600 baud with a 307 kHz carrier.

The problem with the above technique is that a low frequency carrier is preferred to avoid circuit noise problems in the sonobuoy. Also this higher carrier frequency would require the use of higher performance OP-AMPS (more expensive) to produce the same amount of gain at this higher frequency. The distance between the aircraft R/Ts and the MODEM is on the order of 50 feet: therefore, it is preferred to use a phototransistor detector which produces a higher current to avoid noise pick-up problems on this long wire length. With these problems in mind, a different modulation scheme was pursued.

Previous optical communication programs at NADC have used frequency shift keying (FSK) modulation to send voice and data streams with very good results. The modulator is easy to build using a voltage controlled

oscillator (VCO) and the demodulator uses a PLL circuit similar to the ASK demodulator; therefore, the circuitry is simple and the parts count is maintained low. Also a low carrier frequency to bit rate ratio can be achieved which keeps the carrier frequency low yet still results in a high baud rate.

## 5.2 FREQUENCY SHIFT KEYING (FSK) BREADBOARD MODEM

In order to evaluate the recommendations of section 5.1, a circuit was designed to demonstrate that an FSK modulation scheme would work. Also a working FSK system was a good lever to use to force the Navy to re-evaluate the current specification.

Since there were no fixed requirements for the higher baud rate from other projects, it was simply decided to try to design for the maximum baud rate achievable with the currently available hardware. The assumption was that if operation at this high baud rate could be achieved then a slower rate would also be achievable, if not easier to implement. The highest baud rate the portable PC would operate at is 19,200 baud therefore this was the design goal. Simply picking four and five times the baud rate as the two tones, 76.8 kHz

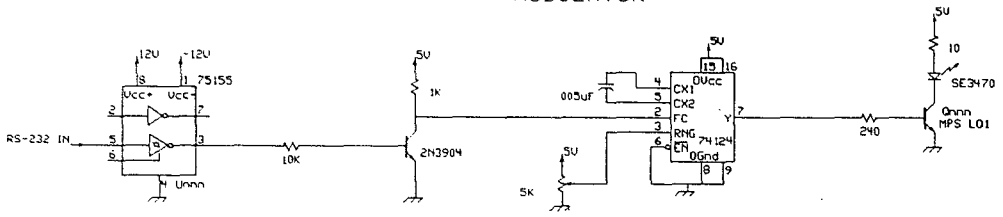
and 96.0 kHz respectively, a circuit was breadboarded (Fig. 10) and evaluated.

The FSK modulator used a voltage controlled oscillator (VCO) integrated circuit, 74124, set up to generate the two FSK tones. The data stream was received with an RS-232 receiver IC and the output was used to drive a transistor switch. This switch was used to drive the frequency control (FC) input of the VCO to switch the output between the two tones. The output of the VCO drives a transistor that switches the IRED on and off at the tone frequency.

The demodulator circuit is somewhat similar to the ASK demodulator circuit in that a PLL circuit is used to detect, in this case, two different tones and demodulate the data stream. Because the carrier frequencies are now higher than phototransistors normally operate, a photodiode was used as the detector. The signal was amplified with a simple inverting OP-AMP circuit with a gain of 10 and capacitively coupled into a PLL IC, LM-565. The PLL VCO free running frequency ( $f_0$ ) is set to operate at the midpoint between the two tones (86.4 kHz). The outputs of the PLL are a reference voltage signal (Pin 6), and an error signal whose amplitude is

REVISIONS		
NO.	DESCRIPTION	DATE
1		

### MODULATOR



### DEMODULATOR

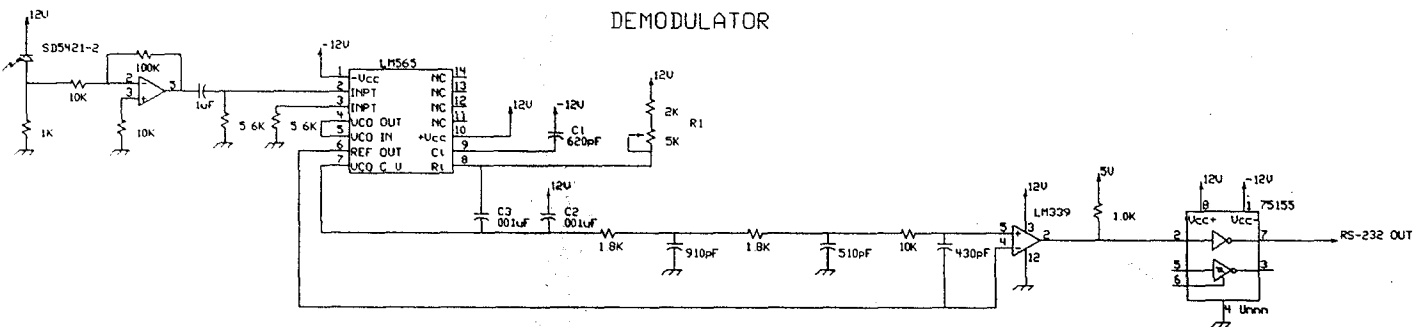


Fig 10 - 19,200 Baud FSK Modem  
78

PREPARED CHECKED ASSISTANT		NATIONAL AIR DEVELOPMENT CENTER HARRISBURG, PA 17027 OPTICAL REMOTE FUNCTION SELECT 19.2 KBAUD FSK MODEM WREARBOARD CIRCUIT	
GELATKA 03-08/91		size code id drawing no no. LEHDWG-FIG10 JMG	
SCALE		SHEET	

proportional to the frequency difference between the input signal frequency and  $f_0$  (Pin 7) and is centered about the reference signal. Therefore; all that is required to then demodulate the data stream is to compare the amplitude of these two signals using a voltage comparator circuit. Any signal above  $f_0$  is decoded as a "one" and any signal below  $f_0$  is decoded as a "zero". The capacitors and resistors between the PLL and voltage comparator is a low pass ladder filter used to remove carrier signal noise still impressed on the output signal. The final demodulator stage is simply an RS-232 driver IC required to send the data stream back to the PC.

Because this FSK MODEM circuit, including optical components, was constructed on a breadboard, only simple tests were done to evaluate the concept. As before, BER testing was done, and the system always achieved 0 BER. Even though a less sensitive photodiode was used as a detector, during the "frost" test, the 20 lb bond paper could be inserted between the optical components and the system would still achieve 0 BER. This result could be attributed to the higher IRED drive current plus the lack of any optical windows and the relative closeness (1/2 inch) of the IRED and photodiode. The major improvement

though over the ASK system was the reduction of signal jitter to about 5 uS during data transitions. Once the PLL locks on to the carrier it stays locked on and smoothly tracks the modulated carrier. A turn on transient still occurs when the demodulator first locks on to the carrier, but operationally this problem can be solved by adding a "carrier detect" phase in which the modulator, and of course the demodulator, is turned on in the data idle state a few (10 minimum) cycles prior to transmission of the first word.

### 5.3 THE NEW FSK SPECIFICATION AND ANALYTIC DESIGN

After some discussion with other programs and the NAVAL AVIONICS CENTER, a new specification was decided upon. Because of another requirement, 1200 baud was picked as the data rate. The two FSK tones were chosen as 19,200 Hz for a logic "1" and 28,800 Hz for a logic "0". These tones were chosen for two reasons. First by keeping the carrier frequency low, high sensitivity phototransistors could be used as the detectors. Secondly, the tones were chosen to provide enough frequency separation to allow a higher baud rate. The system baud rate could be increased and even multiple baud rates could be run depending on future requirements.

These tones would easily allow a data rate of 9600 baud, or possibly higher.

The optical components and design are the same as were used in the airborne ASK system; therefore, the analysis will not be repeated. The VCO IC used in the modulator was chosen simply because it was in the inventory and thus may not necessarily be the ideal component for the task. An analysis of the modulator will not be done. The PLL IC characteristics will be analyzed to determine the effects of this component on the demodulator operation.

The first notable difference between the tone decoder and the FSK PLL demodulator is in the minimum detectable signal. The typical detectable signal level for the LM-565 PLL is listed as 1 mVrms and the guaranteed maximum is 10 mVrms. Using the typical values for minimum detectable signal of both decoders, the PLL should have a 26 dB advantage ( $20 \log 20/1$ ) over the tone decoder. Guaranteed specification values still show an 8 dB advantage to the FSK PLL system. This advantage alone shows the benefit of switching to the FSK system.



Next the temperature effects of the device must be evaluated, which include the changes in  $f_0$  and output signal levels, but first the design equations must be solved to determine the free running frequency, the capture range and the lock range.

The free running frequency of the VCO is set by the equation

$$f_0 = 1.2 / (4 R_1 C_1)$$

and should be set approximately half way between the two FSK tones or in this case 24 kHz. (In actuality, the  $f_0$  is set slightly offset from this frequency to avoid output chatter with no input signal.) The change in  $f_0$  as a function of temperature is on the order of 200 ppm/C. and when tested and graphed over the full temperature range this is given as +1% at -55 C. and -1% at +125 C.. This change must be considered when the capture range is calculated.

The next important parameter of the PLL is the capture range, but this is dependent on the lock range which is given as

$$f_1 = +/- 8 f_0 / V_{CC}$$

where  $V_{CC}$  is the total supply voltage or in this case 10 V (+/- 5V); therefore, the  $f_1 = +/- 19,200$  Hz.

The capture range is given as

$$f_c = +/- (1/(2 \text{ Pi})) \times (2 \text{ Pi } f_1/\text{Tau})^{1/2}$$

where

$$\text{Tau} = (3.6 \times 10^3) \times C_2$$

for the  $C_2 = 0.01$  uF (nearest value available at the time), the capture range is approximately +/- 9,200 Hz from  $f_0$ . This value capacitor worked well in the laboratory, but from this result, and considering the effects of temperature on  $f_0$  as calculated above, the capture range should be increased by reducing the value of  $C_2$ . Using a 0.0068 uF capacitor would increase the bandwidth to +/- 11 kHz which would compensate for the temperature drift.

The only other temperature effects that must be considered is the temperature drift between the output ( $V_7$ ) and the reference voltage ( $V_6$ ). This drift, if excessive compared to the output voltage swing caused by

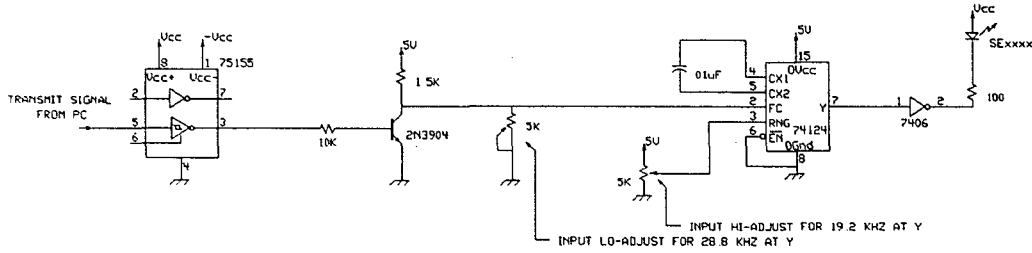
the frequency deviation, can cause errors in demodulating the data stream. The  $V_6 - V_7$  drift is listed as typically 50  $\mu\text{V}/\text{C}$ . which relates to approximately a 5 mV change over the temperature range. Considering a frequency deviation of  $\pm 10\%$  (the ORFS system is  $\pm 20\%$  deviation) is guaranteed to cause a voltage swing of 300 mV P-P, this temperature drift is not a problem.

Now that the design equations have been solved which show the FSK system should work over the full temperature range and sensitivity should be better than the ASK system, a breadboard circuit was built to evaluate these findings.

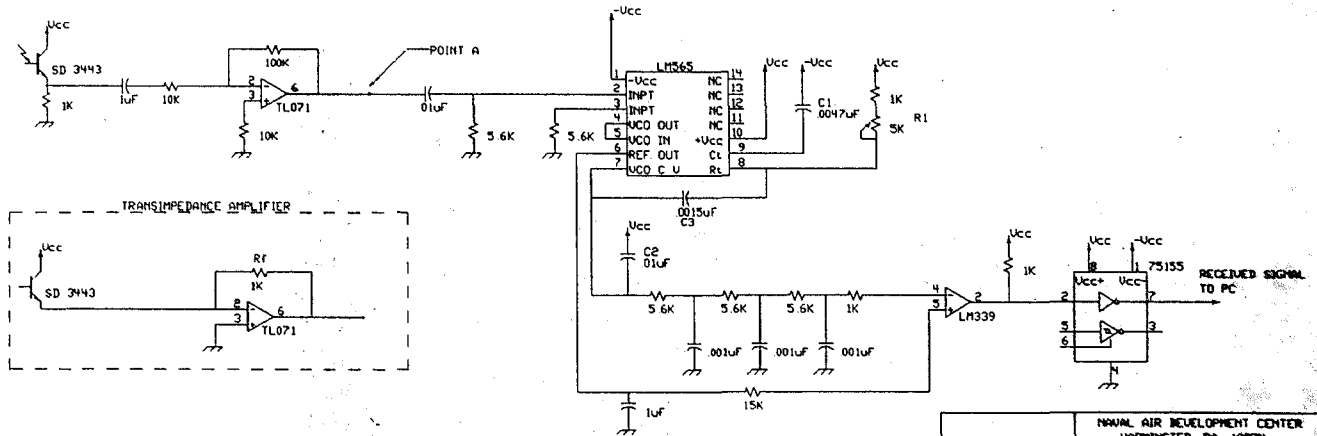
In order to evaluate this design against the proposed specification, the previous FSK breadboard MODEM was modified to operate according to these new requirements. This new FSK MODEM (Fig. 11) is functionally equivalent to the previous design with only some minor changes. Another variable resistor was added to the VCO modulator in order to set the two frequencies easier. Also, as in the ASK modulator, an open collector driver (7406) was used as the IRED driver instead of a transistor.

REVISIONS		
ZONE	DESCRIPTION	DATE APPROVED

### MODULATOR



### DEMODULATOR



- #NOTES  
+Vcc = 5V  
-Vcc = -5V

prepared		size/code id GELATKA 18-24/91	drawing no. LEHMMS-FIG11 BMS
checked			
inspected			
NAVAL AIR DEVELOPMENT CENTER WARMINSTER, Pa. 18074 OPTICAL REMOTE FUNCTION SELECT 1200 BAUD FSK MODEM BREADBOARD CIRCUIT		sheet	sheet

Fig 11 - 1200 Baud FSK MODEM

Because the MODEM now operates at a lower frequency, a phototransistor was used as the receiver detector. Again an inverting OP-AMP circuit with a gain of 10 was used to amplify the signal and a PLL circuit was used to demodulate the signal. The PLL  $f_0$  was again set at half way between the two tones, or 24 kHz. In order to make the circuit operate not only at 1200 baud but also at higher rates, possibly up to 19,200 baud, the output filter bandwidth was designed to accommodate the higher baud rate. The design rule for this filter is that the break frequency should be half way between the highest baud rate frequency (19,200 baud, 9600 Hz) and twice the carrier frequency ( $2 \times 24$  kHz) which turns out to be 28 kHz. Also because the 19,200 baud rate is close to the tone frequencies, two additional low-pass filter stages were added to filter the carrier noise still impressed on the output.

#### 5.4 FSK MODEM TESTING AND EVALUATION

Rigorous testing and signal measurements were done to evaluate not only the circuit design but also the concept. The circuit was constructed on a breadboard which allowed easy changes to the circuit but the disadvantage of a breadboard is that it is also the worst place to build and test an analog circuit. The problems

associated with breadboards include stray capacitance at connections, RF emissions and pick-up on long component lead lengths, plus a lack of a continuous ground plane which usually cause noise problems. These faults usually lead to less than optimum results.

The majority of tests were done to characterize signal levels and receiver sensitivity along with bit error rate testing at various baud rates.

During initial receiver sensitivity tests, one of the first signal discrepancies encountered was a difference in amplitude of the two received tones. At the input to the amplifier the signal level of the 19,200 Hz tone was 1.6 V P-P while the signal level of the 28,800 Hz tone was 1.2 V P-P. This difference is attributed to the response time of the phototransistor. The light current rise time ( $t_r$ ) and fall time ( $t_f$ ) are listed as typically 6  $\mu$ S (80 kHz). The test conditions of this specification are a load resistor ( $R_L$ ) of 1 k $\Omega$ , and a  $V_{cc}$  of 5 V, which the FSK demodulator circuit matches. The timing specifications are referenced at the standard 10% to 90% of output voltage. These switching times appear different than encountered because of the measured signal differences; therefore, phototransistor

response time was investigated and is reported in section 5.5.

As a test, a transimpedance amplifier was constructed and substituted into the FSK demodulator at point A, Fig. 11, to evaluate its use as the phototransistor amplifier. A transimpedance amplifier is sometimes referred to as a current to voltage converter and is commonly used to amplify signals from current output devices such as photodiodes and phototransistors. The gain of the amplifier is set by the value of the feedback resistor. Without going into the detailed circuit analysis, the equation for the amplifier is,

$$V_o = -I_i R$$

or the gain is

$$R = -V_o/I_i \text{ ohms}$$

which is referred to as a transimpedance gain.

The same receiver sensitivity as before could not be attained with this amplifier. To obtain the maximum phototransistor response time, the load resistor

(feedback resistor) is recommended to be 1 kOhm (see section 5.5 for test results). With the frost attenuator, this amounted to 40 mV P-P of signal of the 19,200 Hz tone and only 28 mV P-P of the 28,800 Hz tone output by the amplifier into the PLL. These levels are consistent with the measurements taken at the input to the original amplifier. In order to achieve the gain of 10 of the original amplifier, the transimpedance gain was changed to -10 kOhm. This configuration still would not work even though the signal levels were 500 mV P-P for the 19,200 Hz tone and 300 mV P-P for the 28,800 Hz tone. The problem appeared to be with the quality of the signals. The response time of the phototransistor was severely affected because not only did the output not increase by 10 from the previous configuration, but the output signal was an exponentially shaped triangle wave. The output signal also included -3 V spikes at the switching points which was traced to poor power distribution and could not be fixed on the breadboard. Because of this poor signal quality, the PLL could not lock to the tones and demodulate the data stream. The conclusion therefore is that through proper board layout and construction, the transimpedance amplifier could probably be made to operate, but in itself could not



supply enough gain to achieve the same dynamic range as the simple inverting amplifier.

Converting back to the original amplifier, dynamic range and receiver sensitivity measurements were taken at the 1200 baud data rate. Initially the signal levels at the input to the amplifier were 1.6 V P-P of the 19,200 Hz tone and 1.2 V P-P of the 28,800 Hz tone. The frost simulator was used to quantify typical expected signal loss. With the frost the 19,200 Hz signal measured 37 mV P-P and the 28,800 Hz signal measured 28 mV P-P at the input to the amplifier, which corresponds to a 32 dB loss. At these levels the system still maintained 0 BER.

The same BER testing was done at 2400, 4800, 9600, and 19,200 baud. At the 2400 and 4800 baud rates, no errors were encountered. At 9600 baud some random errors would start to appear and the system would not work at 19,200 baud. The system was then run at 1200 baud and signal measurements were made to track down the cause of the errors. It was suspected that these errors were caused by noise on the outputs of the PLL. The signal output of the PLL would change approximately 450 mV corresponding to the data changes but would have 250 mV P-P of carrier noise on the signal. After the filter

bank, the signal excursion was still about the same and the noise was reduced to 50 mV P-P. The reference signal was stable at 3.7 V but also had 35 mV P-P of noise. The combination of these noise signals would cause the comparator output to chatter and jitter for approximately 10 uS. At 1200 baud this chatter was not a problem because of the relatively long period of a bit time (800 uS).

Knowing this, the system was run at 19,200 baud and the signal measurements were repeated. The outputs of the PLL were approximately the same. After the filters the signal excursion was reduced to 230 mV with 35 mV P-P of noise. The comparator output chatter on average was 15 uS with random spikes out to 25 uS. Because the bit period is now much shorter (50 uS), this causes errors in the UART.

The solutions to this problem would be to filter the noise better or add hysteresis to the comparator circuit. From the above signal measurements, the output filter should not be changed because signal loss is already encountered at the higher baud rate. The noise on the reference signal was highly suspect as the cause of the errors. The addition of the 0.1 uF capacitor reduced

this noise level to 6 mV P-P and the output jitter was reduced to less than 5 uS with little chatter. In this configuration, 0 BER was achieved at 9600 and 19,200 baud without and also with the frost simulator. The fact that such a simple fix solved the problem, a hysteresis circuit was not pursued. Also, this noise problem may not be encountered when good layout and construction practices are adhered to in the final board fabrication.

After this problem was solved, BER testing was done and receiver sensitivity measurements were taken. Minimum signal to maintain 0 BER at 1200 baud was measured at 20 mV P-P of the 19,200 Hz tone and 15 mV P-P of 28,800 Hz tone. This corresponds to 38 dB dynamic range.

As was reported in section 3.3, the beam patterns of narrow beamwidth IREDS are highly irregular. As can be imagined, with each aircraft using 51 R/Ts (48 external loaded launch tubes plus 3 internal loaded launch tubes) and some 200 or more aircraft in the fleet, these irregularities and inconsistencies can cause problems when the ORFS system is installed in fleet aircraft. To investigate if a wide angle beamwidth IRED could be used and still provide similar dynamic range, a 90 degree full

angle IRED (Honeywell SE 3470) was substituted into an R/T assembly. The drive current was measured at 32 mA which corresponds to a total optical power output of 2.2 mW. With no added optical attenuation other than the optical windows, and a 100 Ohm load resistor, the received signal measured 44 mV P-P. This is a 20 dB loss compared to the testing with the narrow transmitter (Section 5.5) in the same configuration. The frost simulator dropped the signal level by 24 dB to 2.8 mV P-P and no errors were encountered at 1200 baud. A signal level of 1.5 mV P-P was required to maintain 0 BER which results in a dynamic range of only 29 dB.

In order to gain dynamic range, the gain of the amplifier was doubled to a gain of 20 and signal measurements were repeated. As was expected, signal levels out of the amplifier doubled, and in this case minimum signal level was about the same (1.4 mV P-P) which results in a 35 dB dynamic range.

A similar result should be achievable by doubling the drive current of the IRED. The IRED is only operating at 32% of recommended output; therefore, 5 dB could be gained just by operating the IRED at the recommended 100 mA drive current.

The allowable angle of misalignment was measured with the frost simulator inserted and it turned out to be +/- 10 degrees. As will be shown in section 5.7, the worst angular misalignment to be encountered was measured at +/- 8 degrees. The conclusion; therefore, is that a wide angle transmitter can operate to 35 dB dynamic range and meet the rotational alignment requirements.

The system was also operated at 19,200 baud data rate. At this rate, the minimum signals out of the amplifier to maintain 0 BER were slightly higher at 32 mV P-P of the 19,200 Hz tone and 28 mV P-P of the 28,800 Hz tone. This still corresponds to a dynamic range of 28 dB.

An interesting observation from the "frost" attenuator is that the actual attenuation varies depending on the optical beamwidths. With the narrow IRED, the attenuation was measured at 36 dB, but only 24 dB loss was measured when the wide beamwidth IRED was used. The obvious explanation for this discrepancy is that the bond paper not only acts as an optical attenuator, but also as an optical diffuser. The paper spreads the optical energy and is dependant on beam

shape. Therefore; optical attenuators such as frost and moisture accumulation on the windows will be hard to characterize but may not be as much a problem as originally expected.

The conclusion of this system testing is that the FSK modulation scheme appears to be a viable technique for the ORFS system. The system could easily achieve 0 BER at 1200 through 19,200 baud data rate. The system also operated with better than 28 dB dynamic range. Of course, these dynamic range numbers mean little until they can be related to actual data that is collected on the expected signal loss that is encountered during typical aircraft operations.

#### 5.5 RESPONSE TIME ANALYSIS AND TESTS

The response times of phototransistors needed to be verified because of the received signal level differences encountered during the previous tests. The manufacturers test circuit was duplicated, which consists of an IRED source and the phototransistor with a 1 kOhm load resistor and a 5 V bias. The distance between the IRED and phototransistor was varied to assess the intensity affects on the response time.

The initial test placed the two device in contact with one another to saturate the phototransistor. In this configuration the rise time of the device was measured at 7 uS which is consistent with the specification. The fall time on the other hand was 80 uS plus another 50 uS from full scale to the 90% value, which is 10 times worse than the specification value. Obviously the load resistor is too high in value to bleed off the accumulated charge of the phototransistor capacitance.

The next step was to separate the devices and determine response times for a typical signal level. The  $t_r$  and  $t_f$  times were then measured at 75 uS. This translates to only a 6 kHz frequency, which supports the signal difference measurements.

Now that the response times were measured and verified as a limiting factor, a technique must be implemented to increase the response times.

First, the equation for rise and fall times must be presented to determine the controlling factors.

$$t_{r,f} = \{(1/2ft)^2 + a(R C G)^2\}^{1/2}$$

where

$f_t$  = Optical input transition frequency

R = Load resistance

C = Collector-base junction capacitance

G = Transistor Gain ( $h_{fe}$ )

a = A constant with value between 4 and 5

From the above equation, the optical input transition frequency which is defined as

$$f_t = 1/(2 t_r)$$

where

$t_r$  = Transmitter response time (0.6  $\mu$ S typically)

is not the limiting factor (700 kHz); therefore, the variables that can be manipulated are G, C, and R.

The gains of the phototransistors are listed from approximately 100 to 900 and the devices are marked with a dash number to indicate the approximate gain of the device. The phototransistor used has the least gain of the device type and therefore has the fastest  $t_r$  and  $t_f$ . Also remember from section 3.1, that as  $h_{fe}$  increases, so



does the dark current which should be minimized to reduce the noise level at high temperature and minimum signal input.

Obviously the junction capacitance affects the rise and fall times. A typical value of 39 pF at 0 V is listed for the device. The junction capacitance though is dependant on the bias voltage. For an abrupt junction phototransistor, the  $C_j$  is proportional to  $V^{-1/2}$ , and for this type of device, which is a graded junction device (planar process), the capacitance is proportional to  $V^{-1/3}$ . Therefore by increasing the bias voltage, the junction capacitance will decrease and the rise and fall times will increase. This technique is not very profitable because by doubling of the bias voltage, the capacitance only decreases by a factor of 0.8. Also, in the aircraft system this would not be a problem, but the sonobuoy is a battery powered device operating at minimum voltage (5 volts). Increasing the voltage to reduce capacitance is not an option.

The only other variable in the above equation that can be changed is the load resistor value. The rise and fall times are directly proportional to the load resistor; therefore, by lowering the load resistor value,

the speed will increase. By reducing the load resistor to 100 ohms,  $t_r$  and  $t_f$  should be on the order of 1  $\mu$ S.

The circuit was modified to use a lower value load resistor to reduce the RC time constant. Simply picking a 100 Ohm load resistor, the test were repeated. At saturation,  $t_r$  was 3  $\mu$ S and  $t_f$  was 11  $\mu$ S with no delay. At the typical signal level,  $t_r$  was 11  $\mu$ S and  $t_f$  was 13  $\mu$ S. These results are still higher than expected, which can be attributed to stray capacitance from the breadboard connections, but these results still show that the system should be able to operate to 40 kHz with little or no signal loss.

Using the above results, the breadboard modem was modified to use the 100 Ohm load resistor. Before this was done, receiver signal measurements were taken for reference. The levels were 1.68 V P-P at 19,200 Hz and 1.14 V P-P at 28,800 Hz . With the modification, the levels were approximately 460 mV P-P at 19,200 and 450 mV P-P at 28,800 Hz. There was still a slight difference between signals, which a good part can attributed to signal measurement errors because of high noise levels. The interesting result is that instead of an expected signal change of 20 dB (factor of 10 change in voltage)

the signal only dropped by 11 db at 19,200 Hz and 8 dB at 28,800 Hz. Obviously the response time of the phototransistor had improved.

The next step was to measure the dynamic range in this configuration. The obvious prediction from the above results is that receiver dynamic range should be decreased by 8 dB. This would not be a significant problem and could be made up by a higher gain in the amplifier. The result turned out to be just the opposite. The system was able to operate down to a 2 mV P-P received signal level, which after the gain of 10 amplifier is a 20 mV P-P signal into the PLL. This corresponds to a 47 dB dynamic range. The PLL therefore responds better to this signal shape which is now more representative of a square wave than the exponential shaped triangle wave as before. In this case, the PLL is operating within the specification value of 1 mVrms (2.82 mV P-P) typical minimum lock-on signal level and 10 mVrms (28.2 mV P-P) guaranteed maximum level for the minimum lock-on signal level.

Of course, this is only one other configuration. When the full system is designed, taking into account all

the cable lengths and wire impedance, more work will have to be done along this line.

#### 5.6 MINIATURIZATION OF RECEIVER/TRANSMITTER

As was reported in section 4.1, the size and weight of the R/T assemblies are of major concern, and an IRED and phototransistor combination device was not suitable for this application. A realizable configuration would be to mount the same type of IRED and phototransistor used previously near to each. In order to do this test, the R/T assemblies were modified. As can be seen in Fig. 12, the IRED (Honeywell SE 5470) and phototransistor (Honeywell SD 3443) were mounted in one holder 5/16 inch apart, center to center, from each other. The IRED and phototransistor now use the same Plexiglass window which reduces the parts count and saves real estate, but creates another problem. The energy from the IRED not only transmits through the window, but also a percentage is reflected at each surface of the window and by each window. As was calculated and measured in section 4.2, this reflection is approximately 8% to 10% total per window. Using the same airborne ASK MODEM with this configuration resulted in poor performance. The system would not work at all because of this self jamming.

TOP VIEW

SLT R/T

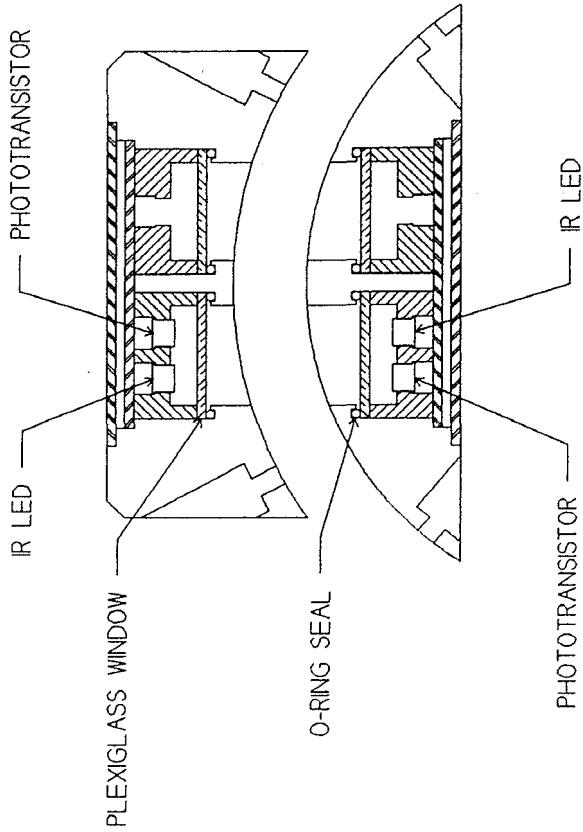


Fig. 12 - Test Fixture Assembly

NAVAL AIR DEVELOPMENT CENTER WRIGHT PATTENSON AIR FORCE TEST FACILITY ASSEMBLY	
DATE	11/27/78
SCALE	AS SHOWN
DWG NO.	ED000Y1012.DWG
REV.	0

The solution to this self-jamming problem is to blank the adjacent receiver during IRED transmissions. The ASK MODEM circuit could not be easily modified to include this feature; therefore, a different approach was used to evaluate this configuration. The wiring was changed to configure the link as a one way link as apposed to the standard bi-directional link. The ORFS system was laboratory tested in this configuration and performance was comparable to the original airborne system.

The result of this experiment is that as long as the adjacent receiver is turned off when the IRED is transmitting and attention is payed to optical beamwidths and clear aperture, there should be no problem shrinking the size of the R/T so that both components operate through the same window.

As a prototype example, a non operational miniature R/T (Fig. 13) was fabricated to demonstrate size and weight savings. This miniature unit is about one quarter the size and weight of the original R/T. Some additional design work still needs to be done on this unit, but this idea was well received and the final product design may well be patterned after this unit.

TOP VIEW

SLT R/T

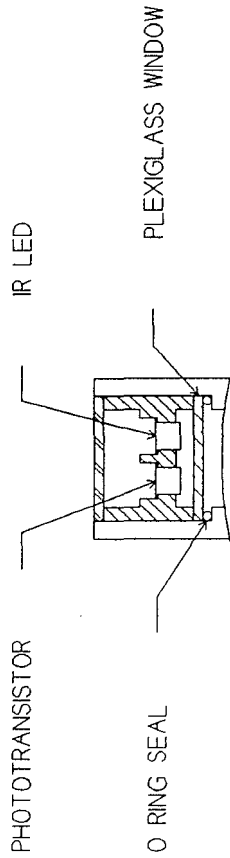


Fig. 13 - Miniature R/T Assembly

NAVAL AIR RESERVE CENTER AVIATION ELECTRONIC CENTER OPTICAL SENSITIVE ELECTRONICS MANUFACTURING ASSEMBLY	
DATE: 11/27/58	DESIGNER: R. J. ...
SCALE:	LEADS: 1/8" DIA.
	DRY:

Another option is to use a IRED and phototransistor in the same package, similar to some laser diode configurations. The design must meet the ORFS requirements. This configuration may already be off-the-shelf and as yet not discovered or the Navy could fund this type of development.

#### 5.7 AIRCRAFT ANGULAR ALIGNMENT MEASUREMENTS

As was reported in section 2.2, there was no specification given for the allowable angular misalignment between the sonobuoy R/T and the SLT R/T. A survey of launch tubes of all U.S. Navy ASW aircraft types was done to investigate this requirement. The largest angular rotation encountered was caused by the use of a small anti-rotation latch of one aircraft type (SH-60B) that would allow the SLC to rotate +/- 8 degrees. The result of this finding showed that the previous designs operated well within this limit and confirmed the optical designs are acceptable and tests were valid. The designs therefore would not have to be re-evaluated. Also, any new optical designs would conform and be tested to this specification.



## 5.8 SECTION SUMMARY

Even though the initial ASK system worked well, there was no capability for future expansion to a higher bit rate. The ASK technique was evaluated and was determined not to be the optimal technique for a higher baud rate. By initially building a breadboard 19.2 kbaud FSK data link, the Navy decided to re-evaluate the specification. A breadboard circuit according to the new FSK specification was constructed to evaluate the specification and was also used to evaluate various components and techniques. Additional testing was done to evaluate optoelectronic devices to improve the response times and thus the dynamic range. A separate task to evaluate a smaller R/T assembly was also done. Most importantly, measurements of aircraft launch tubes were done, so now there is a design specification set for rotational operational limits.

## 6.0 A PRELIMINARY DESIGN FOR THE FULL ORFS SYSTEM

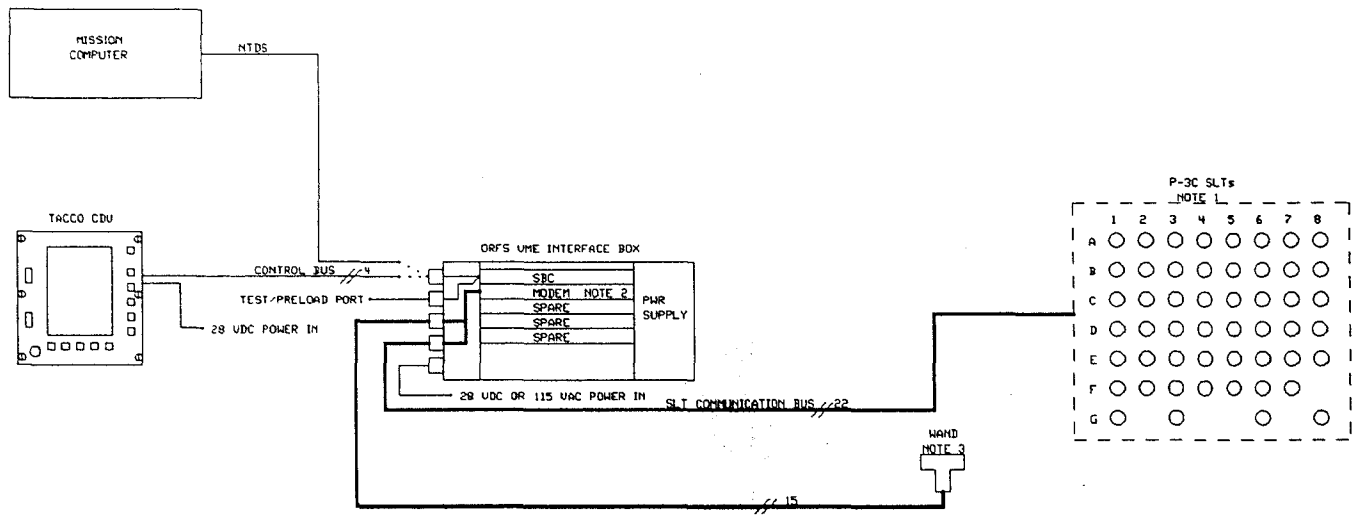
All previous design work for the ORFS system has been geared towards evaluating the concept. Along this line, the system consisted of only breadboard MODEM designs and a single sonobuoy optical link. In order to fully evaluate the entire concept, a complete system design must be developed. This full design is required to uncover any unforeseen technical problems.

A general Navy request is to produce a new system as economical as possible. This requirement can be reached by following two general guidelines. The first guideline is to use off-the-shelf hardware and sub-systems as much as possible. The Navy refers to these as Non Developmental Items (NDI). This design guide saves high non-recurring engineering (NRE) costs associated with designing and testing new Mil-Spec systems. A second way to save engineering costs is to design a system that can be used in as many platforms as possible saving NRE costs required to develop unique systems.

### 6.1 SYSTEM OVERVIEW

A preliminary, high level design of an ORFS system was done and is shown in Fig. 14. The system consists of a computer chassis which houses a single board CPU and

zone		description		revisions	
no.	date	no.	date	no.	date



P-3C SLTs  
NOTE 1

	1	2	3	4	5	6	7	8
A	○	○	○	○	○	○	○	○
B	○	○	○	○	○	○	○	○
C	○	○	○	○	○	○	○	○
D	○	○	○	○	○	○	○	○
E	○	○	○	○	○	○	○	○
F	○	○	○	○	○	○	○	○
G	○	○		○	○		○	○

Fig 14 - P-3C ORFS System Block Diagram

108

- NOTES
1. SEE FIGURE 2 FOR SLT INTERCONNECT
  2. SEE FIGURE 3 FOR MODEM BOARD
  3. SEE FIGURE 4 FOR HAND ASSEMBLY

NAVAL AIR DEVELOPMENT CENTER WARMINSTER, PA 18974		drawing no.	
OPTICAL REMOTE FUNCTION SELECT P-3C AIRBORNE SYSTEM BLOCK DIAGRAM		LEHMING-FIGIN 8MG	
prepared		size	
checked		code	
engineer		id	
GELATKA	09/16/91	no.	
SCALE		sheet	

the custom MODEM card, an operator control unit which can be either a separate control display unit (CDU) or the mission computer systems, and one R/T per launch tube.

The projected computer system would be built according to the Versatile Module European (VME) specifications. This computer architecture is becoming more prevalent in military systems; therefore Mil-Spec certified chassis, computer boards and input/output (I/O) boards are readily available.

The chassis has the room for five cards, but for this case, only room for two cards would be required and the rest of the slots would be available for future expansion. The two cards required for the system are a single board computer (SBC) and the custom MODEM card.

Various SBC cards are available depending on the requirements. Typically the processor for VMEbus systems is based on the Motorola MC680X0 series of microprocessors. For this application, an NDI baseline SBC is all that is required. This SBC would use the MC68020 which is a full 32-bit microprocessor. The baseline memory of 512 kB (kilobytes) of static RAM (Random Access Memory) and 256 kB of EPROM (Electrically

Programmed Read Only Memory) should be plenty of memory for this project considering only simple I/O is required of the computer program and enough RAM memory for the load table is required (approximately 500 bytes).

The SBCs are configured with at least two serial communications ports. One of these ports could be configured as a test/preload port. Through the use of a portable PC, an operator could run test programs to exercise the system to troubleshoot faults.

This port could also be used to automate the initialization of the sonobuoys. A portable PC would load a pre-generated initialization table such that when this function is selected on the ORFS control unit, the sonobuoys will be loaded according to this certain initial configuration. Thus, various initialization tables could be generated at the squadron level on the PC, taking into account local conditions and the mission requirements.

In order for the operator to control the ORFS system, an I/O device is required. For a stand alone system where the ORFS is not integrated with the aircraft systems, a separate CDU could be used. This CDU would

provide the capability to display sonobuoy status and provide the mechanism for the operator to program the sonobuoys as required.

As an option, the ORFS system could be integrated with the mission computer system and avionics. Depending on aircraft type and version, various communications bus structures are used. For the P-3C Update III, the communications bus is the Naval Tactical Data System (NTDS) which is a 32 bit parallel data bus that can operate up to 250,000 words per second. Newer aircraft use the Mil Std 1553 A/B serial data bus. In any case, SBCs are available configured with these various I/O options.

An issue that still needs to be addressed is the communications protocol between the operator control unit and the ORFS system. This I/O is not complicated because of the relatively low number of launch tubes and the limited types of sonobuoys. The proposed message format could just be an expansion of the ORFS sonobuoy programming messages to include a launch tube identification prefix.

## 6.2 THE R/T MATRIX

The major system design that faces the implementation of the ORFS system on an aircraft is how to efficiently connect the R/Ts from all the launch tubes back to the computer chassis. The current systems only used one R/T which required four wires. For the P-3C aircraft, this would translate to 204 wires (51 launch tubes x 4 wires per tube). The wiring complexity and weight alone would prevent the ORFS from ever being accepted into the fleet.

Various techniques were thought of and evaluated to solve this problem. Serial data channels with individual SLT addresses similar to the Mil-Std 1553 data bus were initially considered. The interconnect wiring would be reduced but at the expense of increasing the complexity of the R/T assembly.

A serial bus structure and one discrete select line per each R/T was the next logical step. The R/T would be simple and the wiring would be reduced to 51 select lines plus the serial data channel wiring. Redundancy requirements would require multiple data busses to avoid the possibility of one failure in an R/T or wiring causing the whole system to fail. This technique is

still not optimum, but from an ease of wiring standpoint, may be a viable configuration.

The proposed communication structure would be a matrix format (Fig. 15). The matrix would consist of a column select bus, a receive row bus, and transmit row bus. By selecting a column and selecting the row for the transmit and receive signals, only one R/T would be selected. The actual circuitry to accomplish this and a more in-depth explanation of operation is presented in the next section.

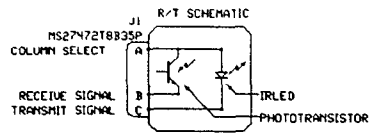
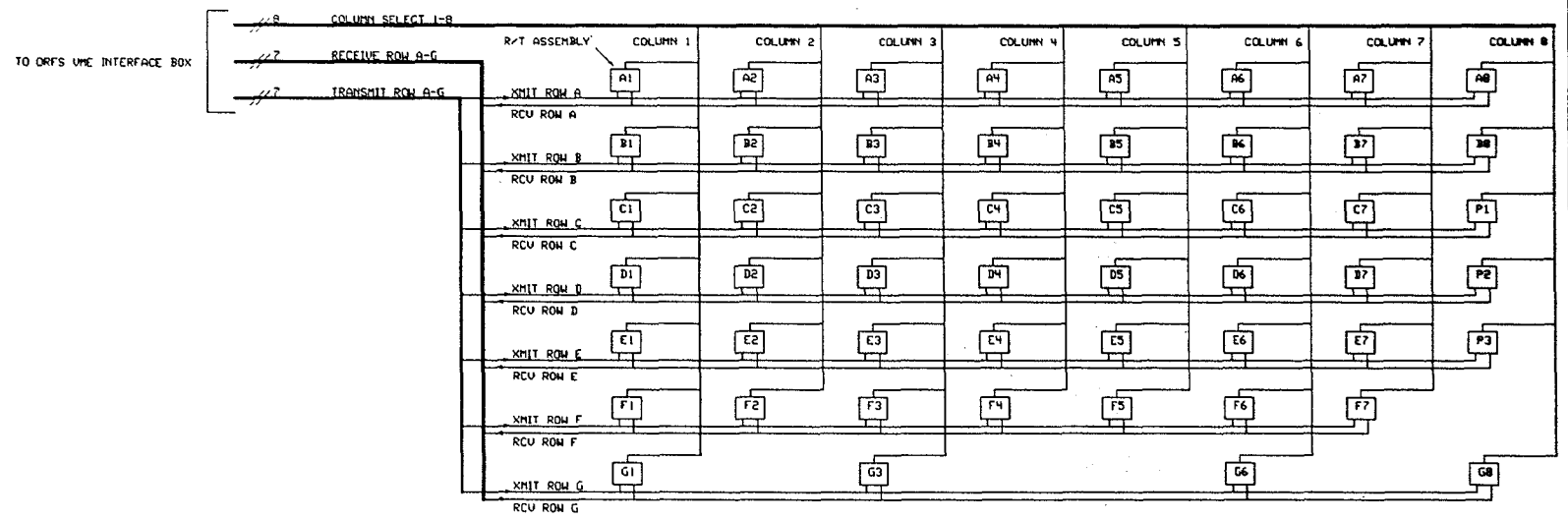
The R/T would simply contain the phototransistor and IRED and no other associated circuitry. The collector of the phototransistor and anode of the IRED are internally connected and wired to a connector pin which would be referred to as the column select pin. The emitter of the phototransistor would be wired to another pin which would be the received signal and the cathode of the IRED to another pin which would be defined as the transmit signal.

This configuration keeps the wiring down to a minimum (22 wires) and minimizes the cost and complexity of the R/T. A very good feature of this technique is



REVISIONS			
NO.	DATE	DESCRIPTION	BY

114  
 FIG 15 - P-3C R/T Matrix Interconnect



DRAWN BY		NOVAL AIR DEVELOPMENT CENTER HARRISBURG, PA. 17034	
CHECKED BY		OPTICAL REMOTE FUNCTION SELECT LAUNCH TUBE R/T INTERCONNECT BLOCK DIAGRAM	
DESIGNED BY		SIZE	CODE
GELATKA 89/06/91		10	10
DATE		DESIGNED BY	DESIGNED BY
89/06/91		LEHNING-FIG15.DWG	
SCALE		SHEET	

that the failure of one R/T does not affect any other R/T. Simply stated, when semiconductor devices fail, they either short circuit or open circuit. If a particular device fails, no other devices in the column are effected because the row signal lines of the failed device are open circuit at the MODEM; therefore, a short or open at the failed device does not affect the rest of the column. Also, a failed device does not affect the other devices in the row because the column select line of the failed device would be open circuit at the MODEM. Of course a single broken wire could cause the loss of a whole row or column, but normally, wires are not prone to breakage.

As a breadboard test, a 4 x 4 matrix of R/T components was constructed complete with column drive transistors, a transmit signal demultiplexer and a receive signal multiplexer. There were no apparent problems encountered with this set-up. Of course in the aircraft system, more attention must be paid to wiring details to prevent electromagnetic interference (EMI) which include interference received on the signal lines as well as interference generated by the system.

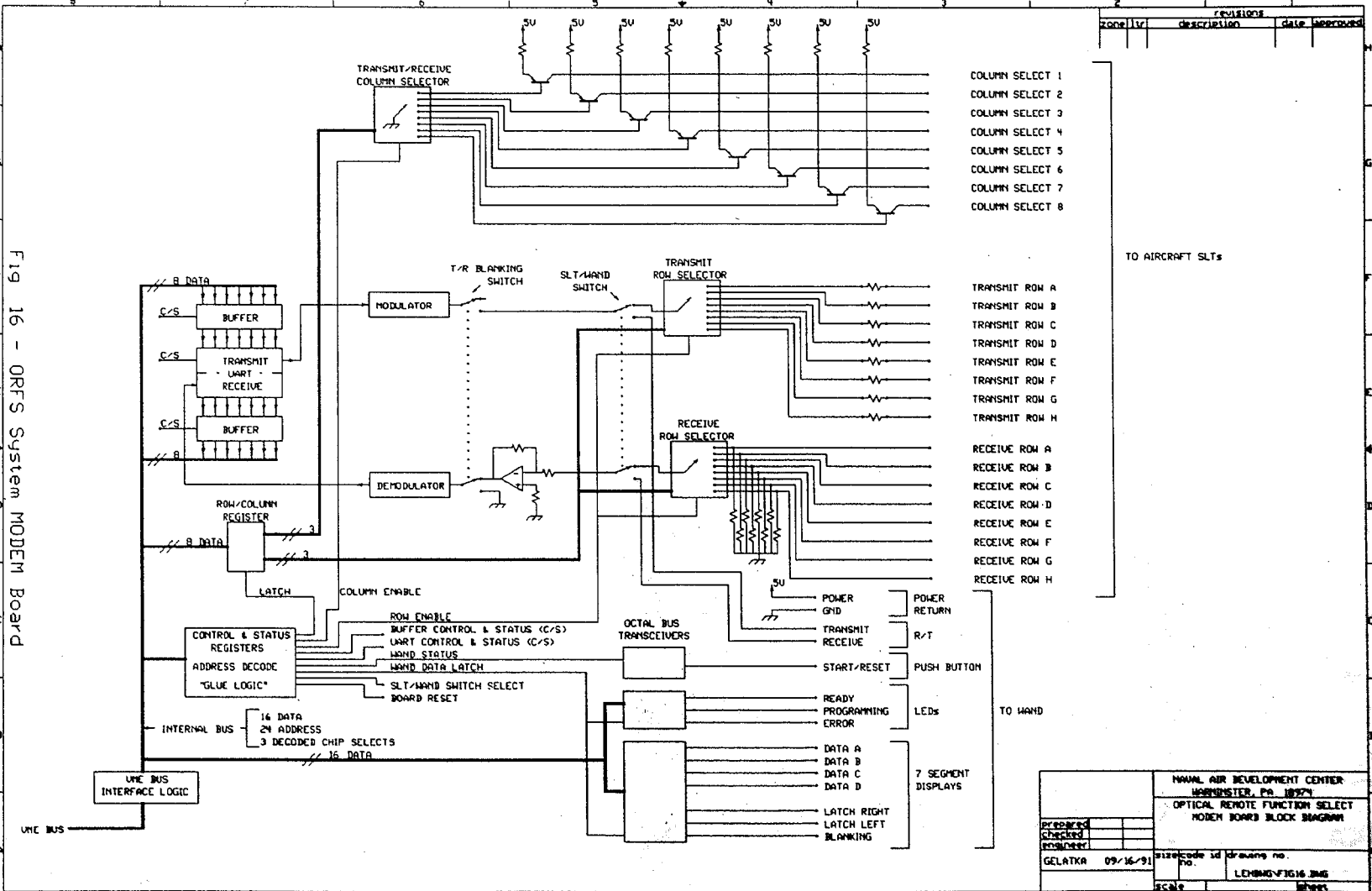
### 6.3 THE ORFS MODEM CARD

The MODEM card (Fig. 16) provides the interface between the SBC and the R/Ts. Through some simple instructions from the SBC, a certain launch tube can be selected and the particular sonobuoy in that tube can be interrogated and programmed. This card would provide the capability to interface to 64 R/Ts. The card could be used by all platforms and the platform would only use as much capability of the card as required. For example, the S-3 requires 60 R/Ts and has no internal stores, the P-3C require 51 R/Ts and plus has internal storage, and helicopters require even less. The design will be described, but only in a high level.

The VMEbus interface logic provides the buffering and interface to the VMEbus which includes a 24 bit address bus, a 16 bit bi-directional data bus, a 16 MHz system clock, plus various interrupt lines and handshake signals. The output of this logic is an internal 16 bit bi-directional data bus, the buffered address bus plus various decoded chip selects and clocks.

The internal bus structure connects to "glue logic" circuits which decode the internal address bus to provide data latches for the various registers and buffers. Two

Fig 16 - ORFS System MODEM Board  
117



REVISED		DATE	APPROVED
Zone	Rev		

- COLUMN SELECT 1
- COLUMN SELECT 2
- COLUMN SELECT 3
- COLUMN SELECT 4
- COLUMN SELECT 5
- COLUMN SELECT 6
- COLUMN SELECT 7
- COLUMN SELECT 8

TO AIRCRAFT SLTs

- TRANSMIT ROW A
- TRANSMIT ROW B
- TRANSMIT ROW C
- TRANSMIT ROW D
- TRANSMIT ROW E
- TRANSMIT ROW F
- TRANSMIT ROW G
- TRANSMIT ROW H
- RECEIVE ROW A
- RECEIVE ROW B
- RECEIVE ROW C
- RECEIVE ROW D
- RECEIVE ROW E
- RECEIVE ROW F
- RECEIVE ROW G
- RECEIVE ROW H

TO HAND

PREPARED CHECKED DESIGNED		NAVAL AIR DEVELOPMENT CENTER WASHINGTON, DC 20330 OPTICAL REMOTE FUNCTION SELECT MODEM BOARD BLOCK DIAGRAM	
GELATKA 09/16/91	size code id drawing no.	no.	LCHMB-FIG 16.005 SHEET

important registers are the control and status registers. The output of the control register is used to control various functions such as selecting column and row of the SLT for communications. The input of the status register is used to monitor the status of various functions, such as the status of the receive and transmit buffers.

The internal data path is used to route data to and from the UART which is used to convert the parallel data to a serial format for transmission and convert the received serial data to parallel. Initially a hardware selected, fixed baud rate UART was envisioned, but because of the capability of multiple baud rates, a software controllable baud rate UART would be used. Because of the high VMEbus bandwidth and slow ORFS baud rate, a buffer for data into and out of the UART would be used to speed match the busses and reduce the waiting time of the SBC. These buffers may be external first-in, first-out (FIFO) buffers or may be internal to the UART depending on which UART is used.

In order to communicate to a specific launch tube, the appropriate column would be selected. The column select transistors switch the voltage on to the selected column. The appropriate row would then be selected for

transmission. The data in the transmit buffer would then be sequentially loaded into the UART and serially sent to the modulator. The modulator would be very similar to the FSK modulator reported on previously. The modulated message would then be routed out through the row selector and out to the transmit row of the selected R/T.

The received message would be routed through the receive row selector, through the demodulator, which again would be similar to the previously designed circuit, and into the UART for serial to parallel conversion. The received parallel data would then be loaded into the receive buffer, and status signals would alert the SBC that data has been received. The T/R blanking switch is shown to point out the requirement of a blanking function, but this function would actually occur in the transmit and receive selector.

An item that has not been described yet, is a hand held wand assembly which would be used to program internal stores, and will be described in the next section. The interface for this wand is also included on the board. The interface consists of some status lines to light certain indicators, control and data lines for

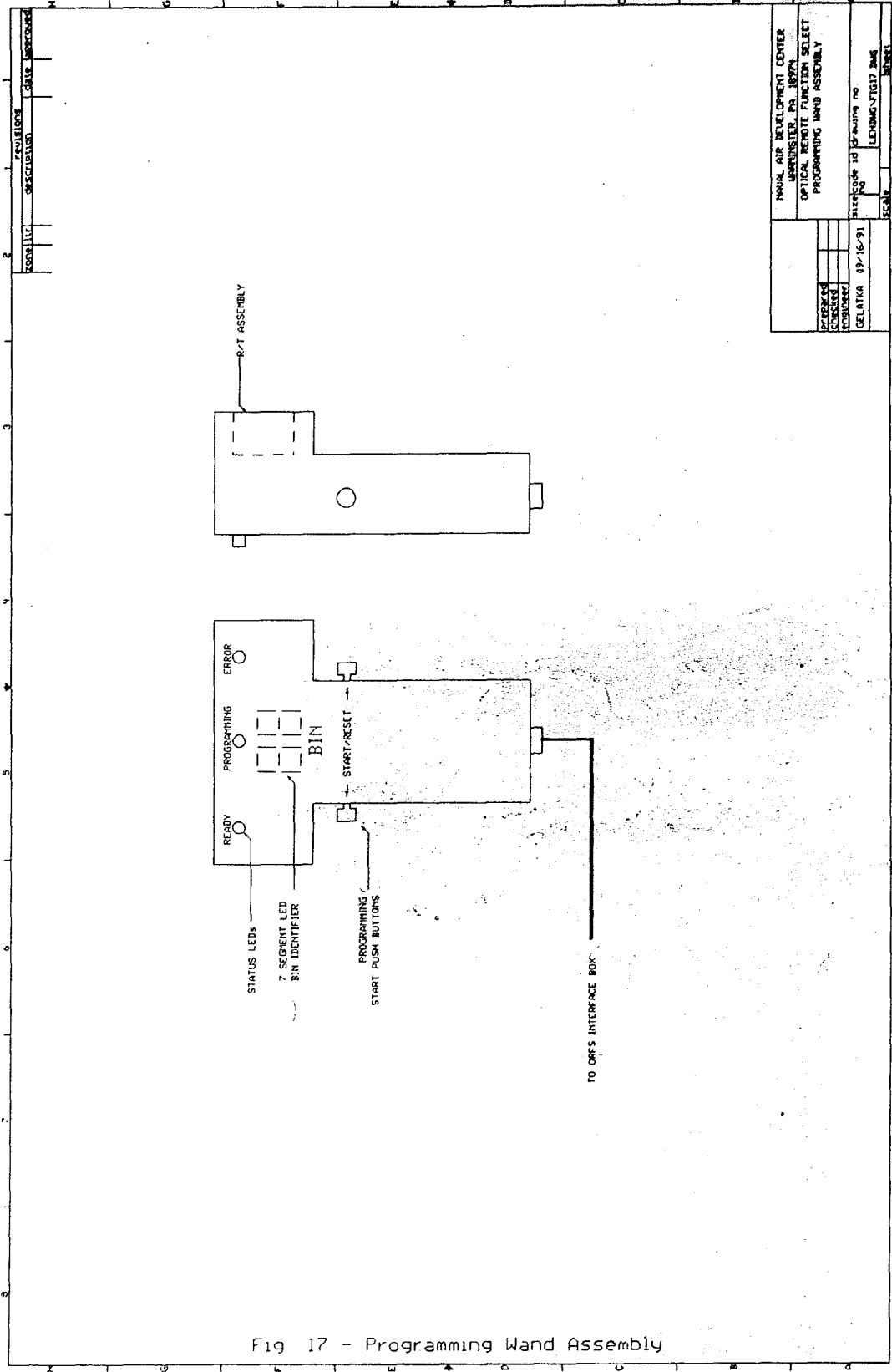
seven segment displays, a start/reset input, and the transmit and receive data lines.

#### 6.4 THE ORFS WAND ASSEMBLY

One of the major benefits of the ORFS system is the capability for automated inventory. There would no longer be any guessing of the amount and type of sonobuoys still available. As was mentioned, the P-3C can carry 36 sonobuoys internal which are launched via one of the three available internally loaded pressurized launch tubes (P-tubes). So far, a technique has not been presented to automatically inventory these internal stores.

It turns out that the bin where the sonobuoy is carried does not provide any positive latching mechanism that would insure alignment of the R/Ts. Therefore; an R/T mounted at each bin would not be feasible, nor would it be required. As a proposed solution, an ORFS wand (Fig. 17) could be developed to provide for semi-automatic programming.

To accomplish the inventory, the wand operator would only have to follow the indicator lights. The TACCO would alert the wand operator and start the internal



NAME: ORS DEVELOPMENT CENTER  
 ADDRESS: PO BOX 1000  
 OPTICAL REMOTE FUNCTION SELECT  
 PROGRAMMING WAND ASSEMBLY

DATE: 09-16-91  
 DRAWING NO: LEDBMC-FIG17 BMS  
 SCALE:

Fig 17 - Programming Wand Assembly



inventory program. The wand 7 segment displays would indicate which bin is requested to be programmed and the ready LED would indicate the ORFS computer is ready to start. The operator would place the wand R/T over the sonobuoy R/T and press the start button. The ORFS computer would light the programming LED and when the reply is received, all displays would blank. If an error occurred during the process, the error indicator would light and would be cleared by the start/reset button so the programming could be tried again..

This wand assembly could also be used to program the sonobuoy prior to insertion into the P-tube for launch.

The advantages of the wand assembly are that now the inventory is accomplished directly with the mission computer and the errors, confusion, verbal communication and time are kept to a minimum.

#### 6.5 SECTION SUMMARY

The whole focus of the Navy's ORFS program has been to evaluate the optical link concept and previous test results have shown that the concept is viable. In order to show that the concept could be extended into a whole

system, a preliminary system design was done and was presented. The system in itself is not very complex but requires careful thought with regards to hardware, communications protocols, and R/T interconnecting wiring. The MODEM design is centered about the previously developed modulator and demodulator circuits with the addition of a VMEbus interface and signal multiplexers and demultiplexers. An added feature is the wand assembly which would allow the ORFS system to operate in a entirely computer controllable, sonobuoy programming and inventory mode. When the Navy gives the go ahead for the system development, more formal design reviews will be done to evaluate the overall design.

## 7.0 SUMMARY

This thesis details the evolution of the ORFS system from development of the initial requirements, through laboratory and aircraft development and testing, through re-evaluation, re-design and testing, right through to a proposed system design. The thesis also detailed the tests done to characterize various components and designs. The results of these tests will be used as a data base for future development.

### 7.1 FINDINGS

The initial ASK modulation was determined to be an acceptable technique for the optical link. The system provided very robust performance at a very simple and inexpensive implementation. If it could be guaranteed that the ORFS system would not be required to operate higher than 300 baud, than this is an appropriate scheme. The problem with the ASK MODEM is the lack of flexibility in increasing the baud rate for future applications. (As a side note, some sonobuoy manufacturers are still requesting that the SPD-22 specification be changed back to the original version and the ASK being the accepted technique because of the simplicity in implementation. This issue is still somewhat open.)

The FSK modulation technique is the preferred scheme for this task. This modulation technique provided the highest dynamic range, even though the circuit was built on a noisy breadboard. With attention to good board design and construction, the MODEM should have no trouble operating at 0 BER at the 1200 baud specification value and could also provide the capability to operate up to 19,200 baud.

Various optoelectronic components were tested, and recommendations were given to which devices provided the best dynamic range plus tolerated the expected misalignment. Of course, what is missing is the lack of real world data on the optical attenuation due to environmental and operational conditions. Long term operational testing is the only way only obtain that data.

The proposed system design, though only a high level, showed that there were no insurmountable engineering problems. The designs are relatively straight forward but there are still issues that need to be worked out such as communication protocols, wiring interconnects and of course the man-machine-interface. When and if the Navy releases the system development

money, these details will be worked out and the system design and fabrication will begin.

## REFERENCES

- Carter Rubber Company. Handbook of Chemistry and Physics. Cleveland, Ohio: CRC Press, 1976.
- Comer, D.J. Modern Electronic Circuit Design. Reading, Massachusetts: Addison-Wesley Publishing Company, 1976.
- Halliday, D., and Resnick, R. Fundamentals of Physics. Revised Printing. New York: John Wiley & Sons, Inc., 1976.
- Honeywell (1990), Honeywell Optoelectronics Data Book. Honeywell Optoelectronics.
- National (1986), National Semiconductor Linear Applications Handbook, National Semiconductor Corporation.
- National (1987), National Semiconductor Linear Data Book Vol. 3, National Semiconductor Corporation.
- Naval Avionics Center. SPD-22 Requirements for the Remote Function Select. Indianapolis, Indiana: Naval Avionics Center, 3 January 1990
- Naval Avionics Center. Revisions to NAC SPD-22. Indianapolis, Indiana: Naval Avionics Center, 30 April 1991.
- Sharp (1990), Sharp Optoelectronics Data Book, Supplementary Edition. Sharp Corporation.
- Siemens (1985), Siemens Optoelectronics Catalog, Siemens Components, Inc.
- Signetics (1974), Signetics Data Book, Signetics Corporation.
- Wilson, J., and Hawkes J.F.B. Optoelectronics, an Introduction. Englewood Cliffs, New Jersey: Prentice Hall, 1983.
- Wojslaw, C.F., and Moustakas, E.A. Operational Amplifiers. New York: John Wiley & Sons, Inc., 1986.
- Ziemer, R.E., and Tranter, W.H. Principles of Communications Systems, Modulation, and Noise. Boston: Houghton Mifflin Company, 1976.

## "VITA"

Mr. Gelatka was born in Pittston Pennsylvania on August 20, 1956 to Mr. William J. Gelatka and Lucille Gelatka (nee Vaxmonsky). He attended Pennsylvania State University majoring in Electrical Engineering and was a member of the Eta Kappa Nu electrical engineering honor society. Mr. Gelatka graduated with a B.S. degree in E.E. 1978 and was, and still is, employed by the Naval Air Development Center (NADC), Warminster, Pennsylvania.

Mr. Gelatka's primary experience at NADC include the development of airborne data acquisition systems for various laser and Magnetic Anomaly Detection (MAD) anti-submarine warfare (ASW) research programs. Mr. Gelatka was also a member of a team which developed a phased array Radar system at NADC in which each team member received a Certificate of Commendation award from the Office of Naval Research (ONR) for "significant accomplishments in the Navy's exploratory development program".

END

OF

TITLE